ELSEVIER

Contents lists available at ScienceDirect

Expert Systems With Applications

journal homepage: www.elsevier.com/locate/eswa





A dynamic cooperative lane-changing model for connected and autonomous vehicles with possible accelerations of a preceding vehicle

Zhen Wang a,b, Xiangmo Zhao a, Zhiwei Chen b,*, Xiaopeng Li b

- ^a School of Information Engineering, Chang'an University, Xian, Shaanxi 710064, PR China
- ^b Department of Civil and Environmental Engineering, University of South Florida, Florida 33620, USA

ARTICLE INFO

Keywords:
Connected and autonomous vehicles
Lane changing
Cooperative control
Dynamic planning

ABSTRACT

The emerging connected and autonomous vehicle (CAV) technologies offer a promising solution to design better lane-changing maneuvers that can reduce the negative impacts of vehicle lane-changing behavior on traffic operations. Existing studies on this topic have predominantly focused on designing lane-changing maneuvers for a subject vehicle (SV) and typically assumed that a vehicle in the target lane must decelerate to make space for the SV due to safety considerations. Nevertheless, jointly designing the trajectories of the SV and surrounding vehicles and allowing possible accelerations of a preceding vehicle may further alleviate the negative impacts of CAV's lane-changing maneuvers. To investigate this possibility, this paper proposes a dynamic cooperative lanechanging model for CAVs with possible accelerations of a preceding vehicle. This model collects information of the surrounding vehicles and updates the lane-changing decisions for the SV in real time via three steps, namely lane-changing decision making, cooperative trajectory planning, and trajectory tracking. This model applies a linearized vehicle kinematic model to make lane-changing decisions for the SV given the states of the SV and surrounding vehicles, the minimum safety distance, and requirements on the comfort level for passengers. Furthermore, it dynamically designs the longitudinal and lateral trajectories for the SV and surrounding vehicles. Extensive numerical simulation experiments are conducted to evaluate the effectiveness of the proposed model. Results show that the proposed model increases the success rate of the SV's lane-changing maneuvers, smoothens the trajectories of the SV and vehicles in the upstream direction at the cost of a slightly more significant oscillation of the last vehicle in the downstream direction. Overall, the proposed model reduces the negative impacts of lane-changing maneuvers on the surrounding traffic. The results also reveal the robustness of the model performance by varying several key input parameters in the experiments.

1. Introduction

Connected and autonomous vehicles (CAVs) have been regarded as a crucial component for the next generation transportation systems due to their substantial potential benefits such as in terms of mobility, traffic emissions, and public health outcomes (Fagnant & Kockelman, 2015; Zhang & Zhu, 2019; Martín et al., 2016). These potential benefits can be achieved primarily because different from human-driven vehicles (HVs), the driving maneuvers of CAVs, such as car-following, lane-changing, and turning, can be relatively accurately designed and controlled. For example, a number of studies have investigated the opportunity of optimizing trajectories of a stream of CAVs to achieve goals such as minimizing the overall fuel consumption or safety risks of the study vehicles (e.g., Li & Li, 2019; Li & Zhou, 2017; Ganji et al., 2014). Among

these maneuvers, lane-changing is particularly important since extensive studies on traditional HV traffic have revealed that improper lane-changing behavior causes traffic oscillation (Pan et al., 2016; Li & Sun, 2017; Li et al., 2015), such as stop and go, traffic congestion, and changes in vehicle speed, and is responsible for 4–15% of accidents (Ammoun, Nashashibi & Laurgeau, 2017). Fortunately, the emerging CAV technologies offer a promising solution to these issues (González et al., 2017). With real-time information of surrounding vehicles (e.g., position, speed, acceleration), a CAV can properly determine its lane-changing decisions (i.e., when and how to change lane) such that the resulting interruption in the traffic operation of the target lane can be reduced.

Inspired by this concept, studies have been conducted to investigate the lane-changing decisions in a CAV environment in the past decades

E-mail addresses: zhenwang@chd.edu.cn (Z. Wang), xmzhao@chd.edu.cn (X. Zhao), zhiweic@mail.usf.edu (Z. Chen), xiaopengli@usf.edu (X. Li).

^{*} Corresponding author.

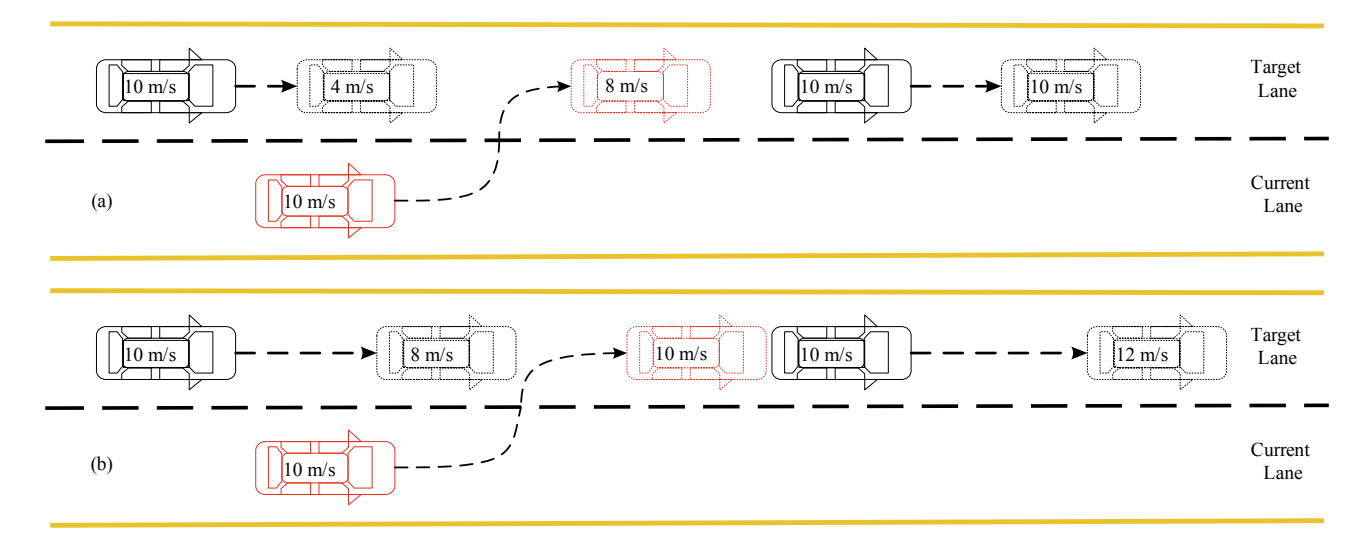


Fig. 1. Two cooperative lane-changing maneuvers. (a) The existing paradigm that requests a following vehicle to decelerate. (b) The proposed paradigm that allows a following vehicle to decelerate and a preceding vehicle to accelerate. Vehicles in solid lines represent the situation before lane changing, and those in dashed lines represent the situation after lane changing.

(Hou, Edara & Sun, 2015; Peng et al., 2020; Tang et al., 2018). Specifically, these studies aim to search for a safe and comfortable lanechanging strategy for a subject CAV that needs to move from a current lane to a target lane given information of two vehicles in the target lane, as shown in Fig. 1(a). Both centralized (i.e., where lane-changing decisions of vehicles in a study system are designed by the subject vehicle; Li, Zhang, Ge, Shao & Li, 2017) and decentralized (i.e., each vehicle decides its lane-changing maneuvers independently; Li, Zhang, Feng, Zhang, Ge & Shao, 2018) lane-changing strategies have been considered. All CAVs determine their lane-changing decisions and generate their trajectories independently in the decentralized lane-changing strategies, which usually results in a lower computation burden. However, due to the time delay in the vehicle-to-vehicle (V2V) communication, the decentralized lane-changing control spends more time negotiating with other CAVs and can be easily trapped in a communication deadlock. On the contrary, the centralized lane-changing control is much more effective, does not cause the communication deadlock, and can achieve system optimum. Further, these studies have also investigated different types of lane-changing contexts (Rahman et al., 2013; Tang et al., 2019), including mandatory (where a vehicle must change lane to reach its destination), discretionary (where a vehicle takes lane-changing maneuvers to achieve a faster speed), and random (where a vehicle's lane-changing decisions do not follow a specific rule). Results from simulation and/or field tests show that the various approaches proposed in these studies are effective in designing CAVs' lanechanging maneuvers under different contexts. Please refer to Rahman et al. (2013) and Wang et al. (2019) for a comprehensive review of this topic.

Despite these methodological advancements, previous studies have primarily focused on developing safe and comfortable lane-changing strategies for CAVs given information of the surrounding vehicles. Depending on whether the surrounding vehicles are cooperative with the subject vehicle or not, existing strategies can be divided into cooperative strategies and uncooperative strategies. In a cooperative lane-changing model, the surrounding vehicles coordinate their behaviors to meet the subject vehicle's need for lane changing (You et al., 2015; Li et al., 2018; Wang et al., 2014a, 2015). For example, a vehicle in the target lane will decelerate to make space for the subject vehicle to change its lane. In contrast, a subject vehicle must wait until there is enough space before lane changing in an uncooperative model since there is no coordination between the subject vehicle and the surrounding vehicles; this is essentially similar to HV traffic (Wang et al., 2014b,

2015). The cooperative strategies have been shown to result in more sensible lane changing decisions and thus to bring better performance for a transportation system overall (Nie et al., 2016). However, studies on cooperative lane-changing models for CAVs are relatively scarce (Luo et al., 2016) and have mostly concentrated on designing lane-changing maneuvers for the subject vehicle while the surrounding vehicles have not received much attention. Thus, the lane-changing behavior of CAVs still causes traffic disruptions (e.g., possible frequent sharp decelerations). This issue can be further addressed by also designing trajectories of the surrounding vehicles under a fully cooperative CAV environment (Wang et al., 2015). This way, the trajectories of the surrounding vehicles can be coordinated with that of the subject vehicles and thus be designed in a way that causes fewer negative impacts to the system overall. Thus, it is necessary to propose a cooperative lanechanging model that simultaneously determines the trajectories of the subject and surrounding vehicles in a fully connected and automated environment, but this topic has not been well investigated.

Further, previous studies have typically assumed that a vehicle in the target lane must decelerate to make space for the subject vehicle for safety considerations, as Fig. 1(a) shows, and otherwise, the lanechanging maneuver cannot be completed. This deceleration process inevitably disrupts the traffic on the target lane despite the properly designed lane-changing maneuvers for the subject CAV. Worse still, the disruption is usually amplified along traffic corridors (e.g., highways) with heavy traffic because the deceleration impacts can be propagated backward in space (commonly known as shockwave in traffic flow analysis); operations of the vehicles in the upstream direction of the following vehicle is likely to be affected. Thus, should their lanechanging maneuvers be realized completely or partially without this deceleration process, CAVs could further decrease the disruption in the existing traffic caused by their lane-changing behavior. One simple solution to this challenge is that apart from requesting a following vehicle to decelerate, a preceding vehicle on the target lane can also accelerate to make space for the subject vehicle, if possible, as shown in Fig. 1(b). This acceleration process only affects the preceding vehicle itself but not the following vehicle and those behinds, thus bringing fewer disruptions to the traffic flow on the target lane. Simple as this idea is, existing studies have predominantly focused on requesting a following vehicle's deceleration (we name this as the "deceleration-only" paradigm hereafter) while a paradigm that allows a following vehicle to decelerate and a preceding vehicle to accelerate (we name this the "accelerationdeceleration" paradigm hereafter) has rarely been investigated.

Table 1 Notation list.

Notation	Description	
С	Vehicle length	m
[0, T]	Time horizon for lane-changing	s
$t \in [0,T]$	Time index	s
$\mathscr{M} = [1, 2, \cdots, \mathit{M}]$	Set of time steps in the lane-changing model	N/A
$m \in \mathscr{M}$	Time step index	N/A
$\mathcal{N} = \{1, 2, \cdots, N\}$	Set of all vehicles considered in the lane-changing model	N/A
$n \in \mathscr{N}$	Vehicle index	N/A
t_m^S	Starting time of the <i>m</i> -th time step	s
$t_m^{ m F}$	Ending time of the <i>m</i> -th time step	s
$u_n(t)$	New input after linearization (i.e., the brake/ acceleration input)	N/A
$v_n(t)$	Speed of vehicle n at timet	m/s
$\theta_n(t)$	Heading of vehicle n at timet	0
$x_n(t), y_n(t)$	Lateral and longitudinal position of vehicle n at time t	m
$a_n(t)$	Acceleration of vehicle n at time t	m/s^2
$a_n^{L}(t)$	Lateral acceleration of vehicle n at timet	m/s^2
$a^{L,MAX}$	Maximum lateral vehicle acceleration	m/s^2
a^{MAX}	Maximum vehicle acceleration	m/s^2
$b^{ m MAX}$	Maximum vehicle deceleration	m/s^2
τ	Inertia delay	s
k_1, k_2	Parameters of the linearized car-following model	N/A
$k_3(m), k_4(m), k_5(m), k_6(m)$	Parameters of the cubic polynomial curve in the <i>m</i> -th time step	N/A
g^{T}	Desired time gap in the linearized car-following model	s
$S^{ ext{MIN}}$	Minimum safety distance	m

^{*} Units of the parameters/variables should be converted to the ones listed in this column before running the proposed model.

Therefore, studies on lane-changing models utilizing the acceleration-deceleration paradigm are needed to further amplify the positive traffic impacts of CAVs via lane-changing maneuvers.

To address these gaps, this paper proposes an innovative dynamic cooperative lane-changing model for CAVs with the proposed acceleration-deceleration paradigm. This is a real-time control model that collects information and update lane-changing decisions for the subject CAV during its operations. The model consists of three primarily steps, including lane-changing decision making, cooperative trajectory planning, and trajectory tracking. Different from previous models, this model jointly considers the subject vehicle and its surrounding vehicles to cooperatively design their trajectories in a dynamic and centralized way. Furthermore, apart from the deceleration of a following vehicle, it

incorporates possible acceleration of a preceding vehicle on the target lane to make space for the subject CAV's lane-changing maneuvers. The contributions of this paper are threefold. First, we propose a new dynamic cooperative lane-changing strategy under a fully CAV environment where a following vehicle and a preceding vehicle can cooperate for the subject vehicle's lane-changing maneuver via deceleration and acceleration, respectively. Allowing a preceding vehicle to cooperate via acceleration produces a higher chance for successful lane-changing maneuver, as well as mitigates the adverse impacts (e.g., traffic disruption) of lane changing on the traffic operation. Second, we propose a dynamic cooperative lane-changing model for CAVs with the acceleration-deceleration paradigm. The proposed accelerationdeceleration paradigm makes traditional lane-changing models not directly applicable. Thus, this model incorporates a lane-changing decision-making approach based on vehicle kinematics and a cubic polynomial curve-based trajectory planning approach to account for this change. With the methodological innovations, the proposed model can jointly determine the trajectories of both the SV and the surrounding vehicles during the lane-changing process in a dynamic way. Finally, to assess the effectiveness of the proposed lane-changing model, we carried out a series of numerical simulations on a hypothetical two-lane highway. Results show that compared with a traditional lane-changing model, the proposed model results in a higher proportion of successful lane-changing maneuver, and smoother trajectories of the SV and vehicles in its upstream direction. Although the last vehicle in the downstream direction experiences a slightly more evident oscillation due to the cooperative acceleration, an overall improvement in all vehicles involved in the lane-changing process can be achieved. The results also reveal that the performance of the proposed model is relatively robust despite variations in several key input parameters. To sum up, this study offers an innovative solution to further reducing the negative impacts of lane-changing behaviors on traffic flow in the future when CAVs are fully deployed. It also provides a simple yet powerful analytical lanechanging model that can be used in CAV studies and planning practice, e.g., being incorporated into simulation software for traffic impact assessment, being used as a prototype for developing more sophisticated dynamic lane-changing models that can be deployed on future CAVs.

The remainder of this paper is organized as follows. Section 2 presents the proposed dynamic cooperative lane-changing model. Section 3 reports results from the numerical simulations to assess the performance of the proposed lane-changing model. Finally, Section 4 briefly concludes this study and discusses future research directions.

2. Dynamic cooperative lane-changing model

This section presents the proposed dynamic cooperative lanechanging model. We first introduce the overall framework of the proposed model and then two key components in the model, a lane-

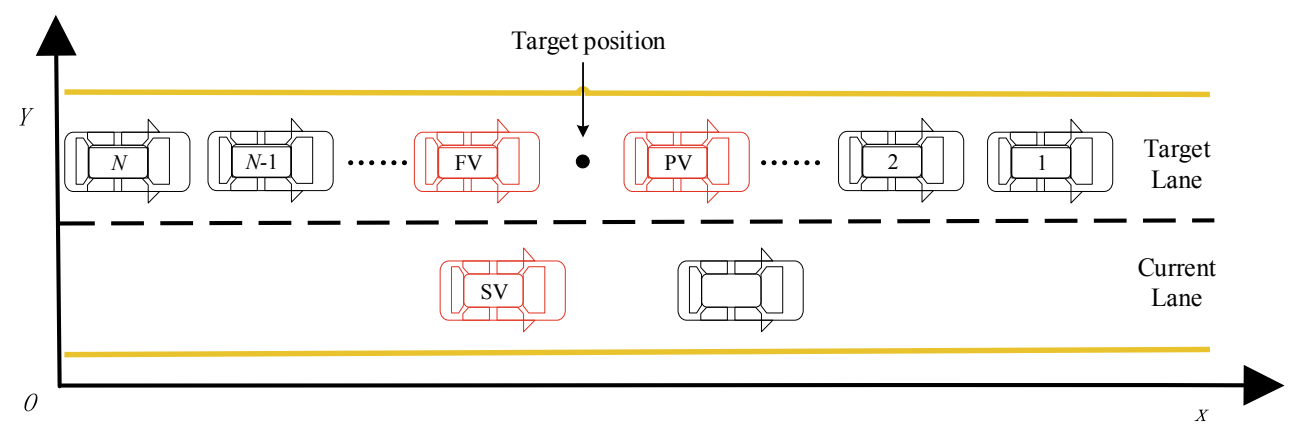


Fig. 2. The investigated traffic system and the study CAVs (vehicles in red) used for analysis.

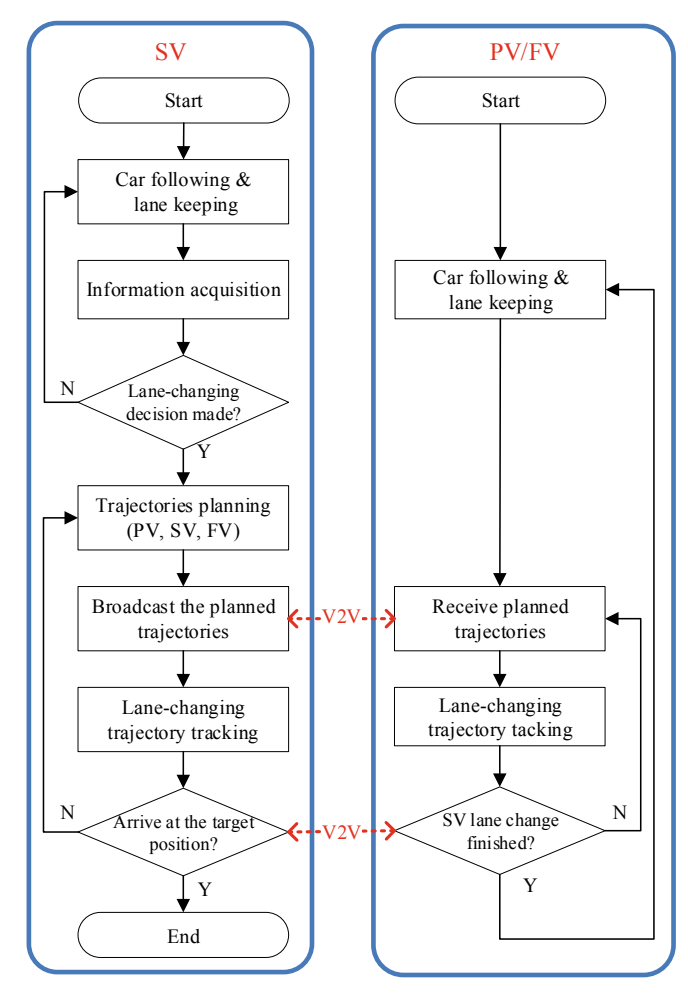


Fig. 3. Framework of the lane-changing model.

changing decision model, and a cooperative trajectory planning approach, will be illustrated in detail. For the convenience of the readers, the key notation used throughout the paper is summarized in Table 1.

2.1. Modeling framework for dynamic cooperative lane changing

This study considers a subject vehicle (SV) \overline{n} that attempts to change lane during a time horizon [0, T], indexed as $t \in [0, T]$, and a set of CAVs $\mathcal{N} = [1, 2 \cdots N]$, indexed as $n \in \mathcal{N}$, on the target lane of the SV, as shown in Fig. 2. Since all vehicles are CAVs, the SV can communicate with its surrounding vehicles and obtain the state of each vehicle $n \in \mathcal{N} \cup \{\overline{n} \text{ at }$ each $t \in [0, T]$, which includes the lateral position $x_n(t)$, longitudinal position $y_n(t)$, speed $v_n(t)$, acceleration $a_n(t)$, and heading (i.e., the direction of vehicle *n*) $\theta_n(t)$. Following previous studies on lane-changing models (Wang et al., 2020), we primarily consider three vehicles in the analysis, the SV, the last preceding vehicle in the downstream direction of the SV's target location on the target lane (PV), and the first following vehicle in the upstream direction of the SV's target location on the target lane (FV), as shown in Fig. 2. For the convenience of the illustration, we call the PV and FV the adjacent vehicles in the following analysis. With the real-time information collected, this study aims to jointly design the behavior of the SV and the adjacent vehicles during the lane-changing process such that the SV's lane-changing maneuvers can be completed in a safe and comfortable manner. Specifically, for the SV, we decide when to change lane and its trajectory during the lane-changing process; for the adjacent vehicles, we design their trajectories to make space necessary for the SV to change lane. Note that the proposed model will

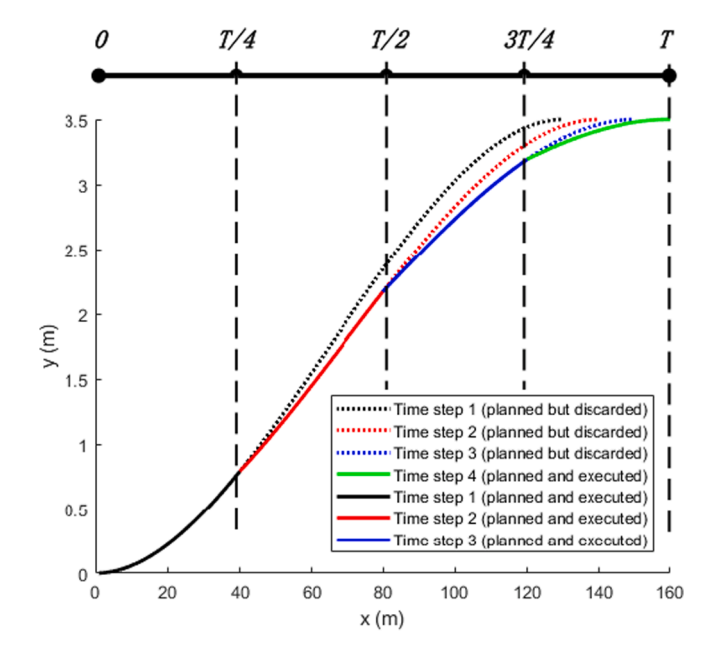


Fig. 4. Dynamic trajectory planning.

be implemented in the SV, and thus the trajectories of all three vehicles are essentially decided by the SV in a centralized control method.

To this end, a dynamic cooperative lane-changing model is proposed, and its framework is presented in Fig. 3. The proposed model primarily consists of four modules, namely information acquisition, lane-changing decision making, cooperative trajectory planning, and trajectory tracking. The information acquisition module collects real-time information of each vehicle during the entire driving process. Once it receives a lane-changing request from the SV, the information collected is fed into the lane-changing decision module to determine whether the SV can change its lane or not; i.e., to determine the starting time and the target position of the SV's lane-changing process. If the SV can change its lane, the cooperative trajectory planning module will be activated immediately to design the trajectories of the SV, PV, and FV for the lane changing process. Otherwise, the model will reenter the information acquisition and lane-changing decision modules until lane-changing is allowable for the SV. Finally, the generated trajectories will be sent to the corresponding CAVs to control their behaviors. While the lanechanging maneuvers are being taken, the trajectory tracking module controls the trajectories of the SV and the adjacent vehicles according to the planned trajectories.

An important feature of the proposed model is that it makes lanechanging decisions and designs vehicle trajectories dynamically. For this purpose, the planning time horizon [0, T] is divided into a set of time steps $\mathcal{M} = [1, 2, \dots, M]$, indexed as $m \in \mathcal{M}$. All time steps are of the same length θ such that $\theta \times M = T$. Note that the length of each time step is dependent on the control period of CAVs' drive-by-wire system, which is usually relatively small values (e.g., 50 ms). With this setting, the lanechanging decision module is activated at the beginning of each time step until an opportunity for cooperative lane-changing is found. Afterwards, the trajectory planning module will start to generate trajectories for the SV and the adjacent vehicles. The generated trajectories will be sent to the relevant vehicles to control their driving maneuvers during the next time step. With real-time inputs form the information acquisition module, the trajectory planning module will generate new trajectories for these vehicles at the beginning of each time step given the change in the traffic condition and the difference between the vehicles' actual and generated trajectories. An example for this dynamic trajectory planning process for a CAV (which can be any vehicle in the study lane-changing system) is shown in Fig. 4. In this example, the time horizon [0, T] is divided into 4 time steps with an equal length of T/4. The curves of different colors represent the trajectories of the CAV planned at the beginning of different time steps. Further, for each curve, the solid section is sent to the CAV for real-time trajectory control while the dashed section is discarded. For example, at the beginning of the first time step (i.e., time 0), a trajectory represented by the black curve is generated for the CAV. The CAV controls its movement according to this black curve while the proposed lane-changing decision model is still running during the first time step. Then, at the beginning of the second time step (i.e., time T/4), a new trajectory represented by the red line is planned and sent to the CAV for real-time control while the old trajectory planned at time 0 (the dashed black curve) is discarded. The process repeats until the end of the time horizon. Thus, the solid sections of each curve constitute the actual trajectory for the CAV's real-time control.

The other key consideration of the proposed cooperative lanechanging model is the surrounding vehicles' willingness to cooperate. Specifically, the SV sends the lane-changing request to its surrounding vehicles via V2V communication. Information in the request includes the SV's position, current lane number, target lane number, and vehicle type (e.g., recreational vehicle, commercial vehicle, emergency vehicle). The PV and FV will then respond to the SV if they are willing to participate in the cooperative lane-changing process or not. If the adjacent vehicles are willing to cooperate with the SV's lane-changing process, their states will then be sent to the lane-changing decision module to check if the SV can safely and comfortably change its lane given the surrounding vehicles' cooperative maneuvers. The possible cooperative maneuvers include the acceleration of the PV and the deceleration of the FV, which have not been jointly considered in the existing lane-changing models for CAVs. In this accelerationdeceleration paradigm, the conditions for the SVs to successfully take lane-changing maneuvers will be changed. Also, the trajectories of both the SV and the adjacent vehicles (i.e., the PV and FV) need to be simultaneously designed. Therefore, new approaches for lane-changing decision making and trajectory planning are needed. Details of the lanechanging decision making and the trajectory planning modules will be provided in the following subsections. Finally, because the proposed dynamic cooperative lane-changing model does not change the vehicle trajectory tracking algorithm greatly, we simply adopt a well-developed algorithm from the existing literature (Li, Sun, Cao, Liu, & He, 2017).

2.2. Lane-changing decision model

We propose a lane-changing decision model to determine if the SV can take lane-changing maneuvers or not. In a fully CAV environment, the lane-changing decision of the SV are subject to the willingness to cooperate of the surrounding vehicles and the safety condition. More specifically, the SV can change lane only if its adjacent vehicles are willing to make space for the SV and there exists a trajectory for the SV's lane-changing maneuver that does not cause longitudinal or lateral collisions between the SV and the adjacent vehicles. The first condition can be determined via V2V communication and negotiation with the adjacent vehicles. Determination of the second condition, however, involves an analysis of the dynamics of the SV and adjacent vehicles. To address the second condition, this section presents an analytical lane-changing decision model based on a linearized vehicle kinematic model. The linearized vehicle kinematic model will first be introduced and then follow the derived lane-changing decision model.

2.2.1. Linearized vehicle kinematic model

To analyze the behaviors of the study CAVs (i.e., both the SV and the adjacent vehicles) for lane-changing decisions, a vehicle kinematic

model is needed. Based on basic physics, the vehicle kinematics can be simply formulated as follows:

$$\dot{x}_n(t) = v_n(t), \forall n \in \mathcal{N}, t \in [0, T]; \tag{1}$$

$$\dot{v}_n(t) = \frac{1}{D_n} \left(P_n \frac{O_n(t)}{R_n} - E_n v_n^2(t) - Q_n D_n g \right), \forall n \in \mathcal{N}, t \in [0, T],$$
(2)

where D_n , P_n , R_n , E_n , and Q_n denote the mass, the mechanical efficiency, the tire radius, the integrated aerodynamic drag coefficient, and the coefficient of rolling resistance, respectively; $O_n(t)$ denotes the actual brake/acceleration torque of vehicle n at time t; and g denotes the acceleration of gravity. Eq. (1) describes the relationship between a vehicle's position and speed while Eq. (2) reveals the relationship between a vehicle's acceleration, mass, and the multiple forces applied on the vehicle

Regardless of its simplicity, the above model is nonlinear in its form, making it difficult to solve these equations directly. For example, the integral operation is needed to compute $x_n(t)$ given the value of $v_n(t)$. Therefore, to achieve a dynamic lane-changing model for CAVs that is suitable for real-time applications, the vehicle kinematic model should be linearized to reduce the computation burden. To this end, we apply the input–output linearization method (Wang et al., 2016; Xiao & Gao, 2011). This method is based on the desired brake/acceleration torque of vehicle n at time t, denoted as $\widehat{Q}_n(t)$, which can be formulated as,

$$\widehat{O}_n(t) = \frac{R_n}{P_n} \left(E_n \left(2\tau \dot{v}_n(t) + v_n(t) \right) + Q_n(t) D_n g + D_n u_n(t) \right), \forall n \in \mathcal{N}, t \in [0, T],$$
(3)

where $u_n(t)$ is the new input after linearization, i.e., the brake/acceleration input, and τ is the inertia delay. Here the inertia delay in the vehicle dynamics system is considered to make the modeling results closer to the actual vehicle kinematics. Furthermore, the relationship between the actual and desired brake/acceleration torques of vehicle n at time t can be formulated as,

$$\widehat{O}_n(t) = O_n(t) + \dot{O}_n(t)\tau, \forall n \in \mathcal{N}, t \in [0, T].$$
(4)

Integrating Eqs. (1)–(4) yields a linear vehicle kinematic model as follows (Li & Peng, 2012; Stanković et al., 2000),

$$\dot{x}_n(t) = v_n(t), \forall n \in \mathcal{N}, t \in [0, T]; \tag{5}$$

$$\dot{v}_n(t) = a_n(t), \forall n \in \mathcal{N}, t \in [0, T]; \tag{6}$$

$$\dot{a}_n(t) = -\frac{1}{\tau} a_n(t) + \frac{1}{\tau} u_n(t), \forall n \in \mathcal{N}, t \in [0, T].$$
 (7)

Then, given information of vehicle n at time t_1 , i.e., $u_n(t_1), \nu_n(t_1), x_n(t_1), \forall t_1 \in [0,T]$, we can formulate the acceleration, speed, and position of the vehicle at time $t_2 > t_1 \in [0,T]$ with the linearized vehicle kinematic model as follows,

$$a_n(t_2) = \left(1 - e^{-\frac{t_2 - t_1}{t}}\right) u_n(t_1), \forall n \in \mathcal{N}, t_1 < t_2 \in [0, T]$$
(8)

$$v_n(t_2) = v_n(t_1) + \left[(t_2 - t_1) - \tau \left(1 - e^{-\frac{t_2 - t_1}{\tau}} \right) \right] u_n(t_1), \forall n \in \mathcal{N}, t_1 < t_2 \in [0, T]$$
(9)

$$x_n(t_2) = x_n(t_1) + v_n(t_1)(t_2 - t_1) + \left[\frac{1}{2} (t_2 - t_1)^2 - \tau \left(t_1 - \tau + \tau e^{-\frac{t_2 - t_1}{\tau}} \right) \right] u_n(t_1), \forall n \in \mathcal{N}, t_1 < t_2 \in [0, T]$$

$$(10)$$

There have been various linearized vehicle kinematic models in the literature to describe the vehicle kinematic characteristics. As this study aims to propose a lane-changing model for CAVs, the main methodological effort is the development of a lane-changing decision model with the unique considerations (e.g., the possible acceleration of a preceding vehicle) and a proper vehicle kinematic model rather than testing different linearized vehicle kinematic models. Thus, we just select a simple but effective linearized vehicle kinematic model that has been demonstrated with satisfactory performance in previous studies (Ghasemi et al., 2013; Li & Peng, 2012). This model considers major factors that affect the CAVs' longitudinal movements (e.g., vehicle mass, mechanical efficiency). Therefore, it is appropriate for modeling the longitudinal characteristics of CAVs. Further, the model is relatively mathematically simple and therefore enables the elegant analytical solutions that are required by a real-time control model. Nonetheless, we acknowledge that the selected model may not be the best, to determine which an exhaustive comparison among existing models is necessary but is out of the scope of this paper. Additionally, should this be the case, the methodological framework presented in this paper could be applied to derive a lane-changing decision model based on other proper linearized vehicle kinematic models. Thus, the work presented here remains important.

2.2.2. Lane-changing decision model

This section presents a lane-changing decision model based on the linearized vehicle kinematic model. The purpose of this lane-changing process in the next time step. Since this study allows the PV to accelerate to make space for the SV's lane-changing maneuvers, existing lane-changing decision models that do not consider this possibility cannot be directly applied. Therefore, we offer an analytical approach to determining the upper- and lower-bound acceleration of the SV in the following analysis.

a. Upper-bound acceleration of the SV.

We first compute the upper-bound acceleration of the SV, which is constrained by the maximum space that the PV can provide for the SV's lane-changing maneuver. This maximum space is dependent on the position of the vehicle in front of the PV, denoted as PPV, at the end of the planning time horizon and the safety distance between the PPV and PV. Since the lane-changing decision is made at the beginning of each time step and the length of the time step is relatively short (e.g., 50 ms), we treat the speed of the PPV as constant in each time step, i.e., $v_{\text{PPV}}(t) = v_{\text{PPV}}(t_m^S), \forall t \in (t_m^S, t_m^F), m \in \mathcal{M}$. Further, define $x_n(t|m)$ as the expected position of vehicle n at time t predicted at the beginning of time step m. Then the expected position of PPV at the end of the lane-changing process precited at the beginning of time step m can be formulated as,

$$x_{\text{PPV}}(T|m) = x_{\text{PPV}}(t_m^{\text{S}}) + v_{\text{PPV}}(t_m^{\text{S}})(T - t_m^{\text{S}}), \forall m \in \mathcal{M}.$$

$$\tag{11}$$

To ensure that the PV does not collide with the PPV, there should be a minimum (or safety) distance, denoted as S^{MIN} , between them, i.e.,

$$S^{\text{MIN}} \le x_{\text{PPV}}(T|m) - x_{\text{PV}}(T|m), \forall m \in \mathcal{M}.$$
(12)

Further, based on Eq. (10) we obtain,

$$x_{\text{PV}}(T|m) = x_{\text{PV}}(t_m^{\text{S}}) + v_{\text{PV}}(t_m^{\text{S}}) \left(T - t_m^{\text{S}}\right) + \left[\frac{1}{2} \left(T - t_m^{\text{S}}\right)^2 - \tau \left(t_m^{\text{S}} - \tau + \tau e^{\frac{T - t_m^{\text{S}}}{\tau}}\right)\right] u_{\text{PV}}(t_m^{\text{S}}), \forall m \in \mathcal{M}.$$
(13)

decision model is, given the states of the SV and the adjacent vehicles, to determine if the SV can change lane safely and comfortably. The essence of this problem is to check if there exists a trajectory for the SV's lane-changing maneuver that does not cause collisions between the SV and the adjacent vehicles. To this end, we first compute the maximum acceleration (or upper-bound acceleration) of the SV based on the kinematics of the SV and PV. Next, we compute the maximum deceleration (or lower-bound acceleration) of the SV based on the kinematics of the SV and FV. If the upper-bound acceleration is greater than or equal to the lower-bound acceleration, we can find at least one feasible trajectory for the SV to complete its lane-changing maneuver. Otherwise, the lane-changing maneuver cannot be completed safely; the SV will keep following its preceding vehicle and repeat the lane-decision making

Note that in Eq. (13) $u_{\mathrm{PV}}(t)$ is constant in time step m, i.e., $u_{\mathrm{PV}}(t) = u_{\mathrm{PV}}(t_m^S), \forall t \in (t_m^S, t_m^F), m \in \mathscr{M}$. This is reasonable because the length of a time step is decided by the control period of the drive-by-wire system, and therefore the control variables (e.g., acceleration, brake/acceleration output) can be changed only once in each time step. Besides, this treatment will not cause much accuracy loss because the length of each time step is relatively short. The same treatment is applied throughout the remaining analysis in this subsection. Integrating Eqs. (11)-(13) yields the relationship between the theoretical brake/acceleration output of the PV $u_{\mathrm{PV}}(t_m^S)$ and t_m^S as follows,

$$u_{\text{PV}}(t_{m}^{S}) \ge \frac{x_{\text{PPV}}(t_{m}^{S}) + v_{\text{PPV}}(t_{m}^{S})(T - t_{m}^{S}) - S^{\text{MIN}} - x_{\text{PV}}(t_{m}^{S}) - v_{\text{PV}}(t_{m}^{S})(T - t_{m}^{S})}{\left[\frac{1}{2}(T - t_{m}^{S})^{2} - \tau\left(t_{m}^{S} - \tau + \tau e^{-\frac{t_{m}^{S} - t_{m}^{S}}{2}}\right)\right]}, \forall m \in \mathcal{M}.$$
(14)

Applying Eq. (14) into Eq. (8) yields the relationship between the theoretical acceleration of the PV and $t_{s_n}^s$ as follows,

$$a_{\text{PV}}\left(t_{m}^{\text{S}}\right) \geq a_{\text{PV}}\left(t_{m}^{\text{S}}\right)$$

following a similar logic. First, based on the safety condition and Eq. (10) we obtain

$$S^{\text{MIN}} \le x_{\text{PV}}(T|m) - x_{\text{SV}}(T|m), \forall m \in \mathcal{M};$$
(19)

$$= \left(1 - e^{-\frac{T - r_{m}^{S}}{\tau}}\right) \left(\frac{x_{PPV}(t_{m}^{S}) + v_{PPV}(t_{m}^{S})(T - t_{m}^{S}) - S^{MIN} - x_{PV}(t_{m}^{S}) - v_{PV}(t_{m}^{S})(T - t_{m}^{S})}{\left[\frac{1}{2}(T - t_{m}^{S})^{2} - \tau\left(t_{m}^{S} - \tau + \tau e^{-\frac{T - r_{m}^{S}}{\tau}}\right)\right]}\right), \forall m \in M.$$
(15)

To guarantee the passengers in the PV are comfortable during the cooperative lane-changing process, the maximum acceleration of the PV should always be no greater than the maximum comfortable acceleration. Thus, we obtain the realistic maximum acceleration of the PV

$$x_{SV}(T|m) = x_{SV}(t_m^S) + v_{SV}(t_m^S) \left(T - t_m^S\right) + \left[\frac{1}{2}\left(T - t_m^S\right)^2 - \tau \left(t_m^S - \tau + \tau e^{\frac{T - t_m^S}{\tau}}\right)\right] u_{SV}(t_m^S), \forall m \in \mathcal{M}.$$

$$(20)$$

estimated at time step m as,

$$\overline{a}_{\text{PV}}(t_m^S) = \min\left\{a_{\text{PV}}(t_m^S), a^{\text{MAX}}\right\}, \forall m \in \mathcal{M}.$$
(16)

Solving Eqs. (19)-(20) yields

$$u_{SV}(t_{m}^{S}) \geq \overline{u}_{PV1}(t_{m}^{S}) + \frac{x_{PV}(t_{m}^{S}) + v_{PV}(t_{m}^{S})(T - t_{m}^{S}) - S^{MIN} - x_{SV}(t_{m}^{S}) + v_{SV}(t_{m}^{S})(T - t_{m}^{S})}{\left[\frac{1}{2}(T - t_{m}^{S})^{2} - \tau\left(t_{m}^{S} - \tau + \tau e^{-\frac{T - r_{m}^{S}}{\tau}}\right)\right]}, \forall m \in \mathcal{M}.$$
(21)

and

Accordingly, the realistic maximum brake/acceleration output of the PV is,

$$\overline{u}_{PV}(t_m^S) = \begin{cases} u_{PV}(t_m^S) & \overline{a}_{PV}(t_m^S) \le a^{MAX} \\ \frac{a^{MAX}}{\left(1 - e^{\frac{T - t_m^S}{T}}\right)} & \overline{a}_{PV}(t_m^S) > a^{MAX} \\ , \forall m \in \mathscr{M}. \end{cases}$$
(17)

Applying Eq. (17) into Eq. (10) yields the furthest position that the PV can reach during the acceleration process estimated at time step m as With this, we can compute the upper-bound acceleration of the SV

$$\overline{x}_{PV}(T|m) = x_{PV}(t_m^S) + v_{PV}(t_m^S) \left(T - t_m^S\right) + \left[\frac{1}{2} \left(T - t_m^S\right)^2 - \tau \left(t_m^S - \tau + \tau e^{\frac{T - t_m^S}{\tau}}\right)\right] \overline{u}_{PV}(t_m^S), \forall m \in \mathcal{M}.$$

$$(18)$$

$$a_{SV}(t_{m}^{S}) \geq a_{SV}(t_{m}^{S}) := \left(1 - e^{\frac{T - \frac{S}{m}}{r}}\right) \left(\overline{u}_{PV}(t_{m}^{S}) + \frac{x_{PV}(t_{m}^{S}) + v_{PV}(t_{m}^{S})(T - t_{m}^{S}) - S^{MIN} - x_{SV}(t_{m}^{S}) + v_{SV}(t_{m}^{S})(T - t_{m}^{S})}{\left[\frac{1}{2}(T - t_{m}^{S})^{2} - \tau\left(t_{m}^{S} - \tau + \tau e^{\frac{T - t_{m}^{S}}{r}}\right)\right]}\right), \forall m \in \mathcal{M}.$$
(22)

Finally, the upper-bound acceleration of the SV is

$$\overline{a}_{SV}(f_m^S) = \min \left\{ a_{SV}(f_m^S), a^{MAX} \right\}, \forall m \in \mathcal{M}.$$
 (23)

b. Lower-bound acceleration of the SV.

The lower-bound acceleration of the SV is achieved if the FV decelerates with the maximum comfortable deceleration $b^{\rm MAX}$ during the cooperative lane-changing process. Further, the speed of the FV must be a nonnegative value. Therefore, the maximum brake/acceleration output of the FV can be formulated as,

$$\overline{u}_{\text{FV}}(t_m^S) = \begin{cases} b^{\text{MAX}} & v_{\text{FV}}(t_m^S) \ge -b^{\text{MAX}}(T - t_m^S) \\ \frac{v_{\text{FV}}(t_m^S)}{T - t_m^S} & v_{\text{FV}}(t_m^S) < -b^{\text{MAX}}(T - t_m^S) \end{cases}, \forall m \in \mathscr{M}.$$
(24)

The position of the FV at the end of the lane-changing process with the maximum brake/acceleration output estimated at the beginning of time step m is,

constraint, we compute the position of the SV with the maximum theoretical brake/acceleration output as,

$$v_{SV}(T|m) = v_{SV}(t_m^S) + \left[\left(T - t_m^S \right) - \tau \left(1 - e^{\frac{T - r_m^S}{\tau}} \right) \right] u_{SV}(t_m^S), \forall m \in \mathcal{M};$$
(29)

Then the realistic maximum brake/acceleration output of the SV is

$$u_{SV}(t_m^S) = \begin{cases} u_{SV}(t_m^S) & v_{SV}(T|m) \ge 0 \\ -\frac{v_{FV}(t_m^S)}{\left[(T - t_m^S) - \tau \left(1 - e^{-\frac{T - t_m^S}{\tau}} \right) \right]} & v_{SV}(T|m) < 0 , \forall m \in \mathcal{M}. \end{cases}$$
(30)

Applying Eq. (30) into Eq. (8), we obtain the theoretical lower-bound acceleration of the SV as

$$x_{\text{FV}}(T|m) = x_{\text{FV}}(t_m^{\text{S}}) + v_{\text{FV}}(t_m^{\text{S}})\left(T - t_m^{\text{S}}\right) + \left[\frac{1}{2}\left(T - t_m^{\text{S}}\right)^2 - \tau\left(t_m^{\text{S}} - \tau + \tau e^{\frac{T - t_m^{\text{S}}}{\tau}}\right)\right] \overline{u}_{\text{FV}}(m), \forall m \in \mathcal{M}.$$

$$(25)$$

With the safety condition

$$S^{\text{MIN}} \le x_{\text{SV}}(T|m) - x_{\text{FV}}(T|m), \forall m \in \mathcal{M},$$
(26)

and the vehicle dynamic of the SV,

$$a_{SV}(t_m^S) = \left(1 - e^{-\frac{T - I_m^S}{\tau}}\right) u_{-SV}(t_m^S), \forall m \in \mathcal{M}$$
(31)

Taking into account the requirement on the passengers' level of comfort, we obtain the actual lower-bound acceleration of the SV as

$$x_{SV}(T|m) = x_{SV}(t_m^S) + v_{SV}(t_m^S)(T - t_m^S) + \left[\frac{1}{2}(T - t_m^S)^2 - \tau \left(t_m^S - \tau + \tau e^{-\frac{T - t_m^S}{\tau}}\right)\right] u_{SV}(t_m^S), \forall m \in \mathcal{M},$$
(27)

we obtain the maximum theoretical brake/acceleration output of the $\ensuremath{\mathsf{SV}}$ as

$$u_{SV}(t_m^{S}) = \frac{S^{MIN} - x_{FV}(t_m^{S}) - v_{FV}(t_m^{S})(T - t_m^{S})}{\left[\frac{1}{2}(T - t_m^{S})^2 - \tau \left(t_m^{S} - \tau + \tau e^{\frac{T - t_m^{S}}{\tau}}\right)\right]} - b^{MAX}, \forall m \in \mathscr{M}.$$
 (28)

Again, the speed of the SV cannot be a negative value. To apply this

$$a_{-SV}(t_m^S) = \max\{a_{SV}(t_m^S), b^{MAX}\}, \forall m \in \mathcal{M}.$$
(32)

2.3. Cooperative trajectory generation

After making the cooperative lane-changing decision, the proposed model needs to design trajectories for the SV, PV, and FV during the lane-changing process. A vehicle's trajectory can be decomposed into longitudinal and lateral trajectories. For the SV that needs to change its

Table 2Other parameters used in the simulation.

Parameters	Value	Unit	Parameters	Value	Unit
L	3.5	m	$\mathcal{S}^{ ext{MIN}}$	6.0	m
C	4.96	m	g^T	1.5	S
T	6	S	a^{MAX}	1.5	m/s^2
k_1	1.4	s^{-2}	$b^{ m MAX}$	-1.0	m/s^2
k_2	0.85	s^{-1}	$a^{L,MAX}$	1.4	m/s^2

Table 3
Success rates of lane-changing maneuvers from the TLCM and CLCM.

Model	Number of successful lane-changing maneuvers	Success rate of lane-changing maneuvers
TLCM	51,752	53.1%
CLCM	70,756	72.6%

lane, both longitudinal and lateral trajectories should be designed. However, for PV and FV, we simply need to plan their longitudinal trajectories since they will move on the same lane. In the following analysis, we present approaches for generating the longitudinal and

lateral trajectories.

2.3.1. Longitudinal trajectory planning

To reduce the impacts of the lane-changing process on the upstream traffic, the PV will accelerate with its upper bound acceleration $\overline{u}_{\text{PV}}(t_m^S)$, $\forall m \in \mathscr{M}$. The SV and PV will then conduct cooperative car following. To model the car-following behavior, this study applies the linearized car-following model proposed by Milanés and Shladover (2014), one of the popular car-following models for CAVs. Let $\widehat{a}_{\text{SV}}(m)$, $\widehat{a}_{\text{FV}}(m)$ be the target acceleration of the SV and FV during time step m, respectively. Then the car-following behavior of the SV and FV can be formulated as,

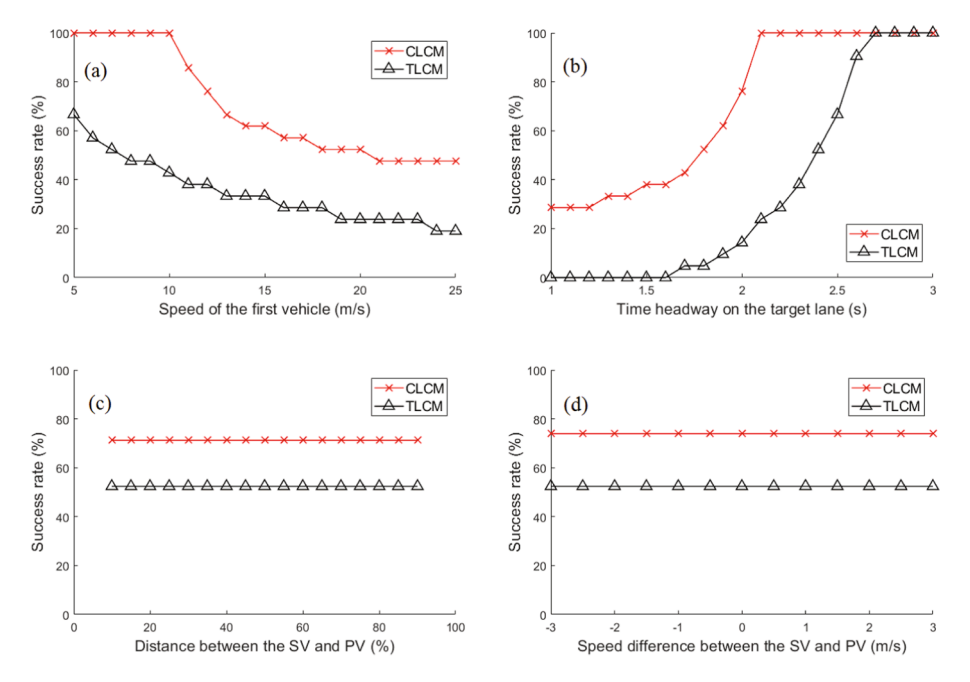


Fig. 5. Success rates of lane-changing maneuvers with (a) varying speed of the first vehicle on the target lane, (b) varying initial time headway between each two consecutive vehicles on the target lane, (c) varying initial distance between the SV and PV, and (d) varying initial speed difference of the SV and PV.

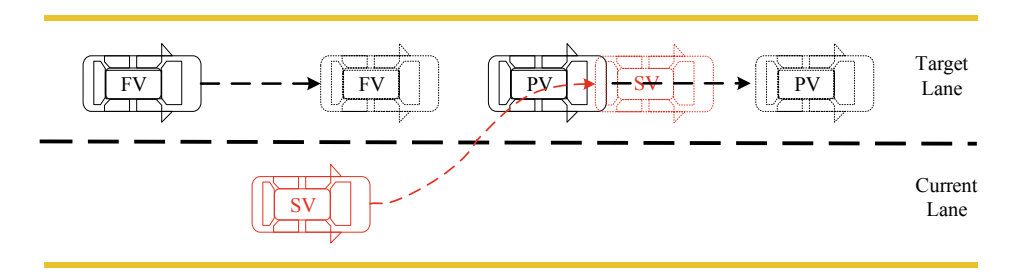


Fig. 6. Lane-changing trajectories of the PV, SV, and FV in one simulated scenario.

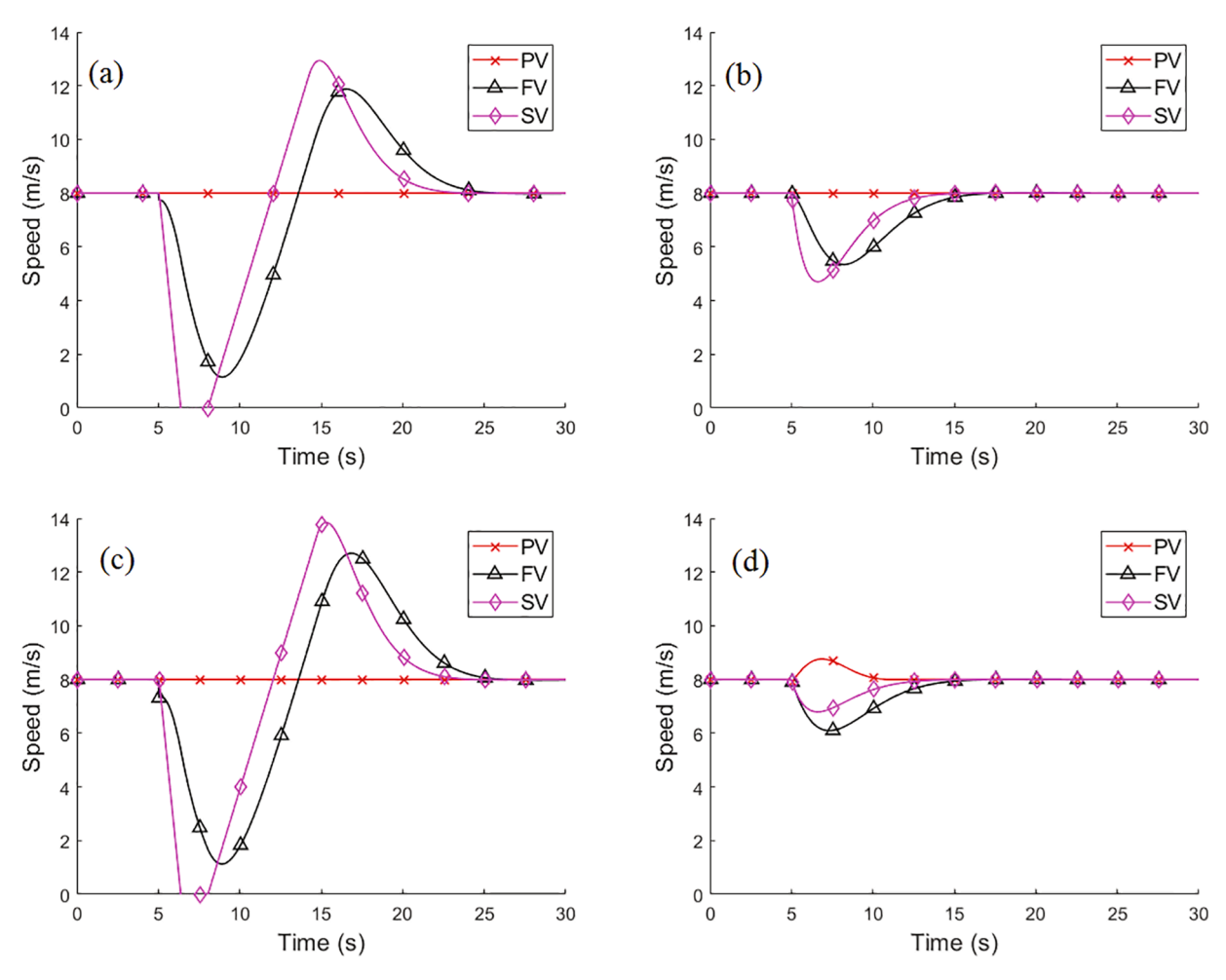


Fig. 7. Speed evolutions of the study CAVs produced by: (a) TLCM in the first representative scenario, (b) CLCM in the first representative scenario, (c) TLCM in the second representative scenario, and (d) CLCM in the second representative scenario.

$$\widehat{a}_{SV}(m) = k_1 \left(x_{PV}(f_n^s) - x_{SV}(f_n^s) - C - v_{SV}(f_n^s) g^T \right) + k_2 \left(v_{PV}(f_n^s) - v_{SV}(f_n^s) \right), \forall m \in \mathcal{M}; \tag{33}$$

$$\widehat{a}_{\text{FV}}(m) = k_1 \left(x_{\text{SV}}(t_m^S) - x_{\text{FV}}(t_m^S) - C - v_{\text{FV}_1}(t_m^S) g^{\text{T}} \right) + k_2 \left(v_{\text{SV}}(t_m^S) - v_{\text{FV}}(t_m^S) \right), \forall m \in \mathcal{M}, \tag{34}$$

where k_1, k_2 are statis known values st, g^T is the desired time gap between the adjacent vehicles. The output from this linearized carfollowing model will be sent to both SV and FV to control their acceleration at each time step.

2.3.2. Lateral trajectory planning

To generate the lateral trajectory of the SV, we apply a cubic polynomial trajectory planning method. The cubic polynomial trajectory rather than other methods such as sine trajectory is selected because its second-order smoothness (Yang et al., 2018) and computational tractability make it appropriate for real-time trajectory planning. The cubic polynomial curve can be mathematically formulated as,

$$y_{SV}(x_{SV}(t)) = k_3(m)x_{SV}(t_m)^3 + k_4(m)x_{SV}(t_m)^2 + k_5(m)x_{SV}(t_m) + k_6(m),$$

$$\forall m \in \mathcal{M}, t \in [0, T].$$
 (35)

As mentioned previously, the state of the SV can be obtained at the beginning of each time step t_m^S , including lateral position $x_{SV}(t_m^S)$, longitudinal position $y_{SV}(t_m^S)$ and heading $\theta_{SV}(t_m^S)$. Further, from the lanechanging decision-making module, we obtain the lateral position of the SV at the end of the time horizon $x_{SV}(T|m)$. Since the SV moves from the center of the current lane to that of the target lane, the horizontal position of the SV at the end of the time horizon is $y_{SV}(x_{SV}(t_m^S)) + L$, where L denotes the width of a single lane. To simplify the computation and expedite the trajectory generation process, we assume that the SV's target heading (i.e., $\theta_{SV}(T|m)$) is 0. Note that one can set $\theta_{SV}(T|m)$) as other desired values and the solution procedure proposed here still applies but with higher complexity. Applying the above information into Eq. (35), we obtain,

$$y_{SV}(x_{SV}(t_m^S)) = y_{SV}(t_m^S), \forall m \in \mathcal{M};$$
(36)

$$y_{SV}(x_{SV}(T|m)) = y_{SV}(x_{SV}(t_m^S)) + L, \forall m \in \mathcal{M};$$

$$(37)$$

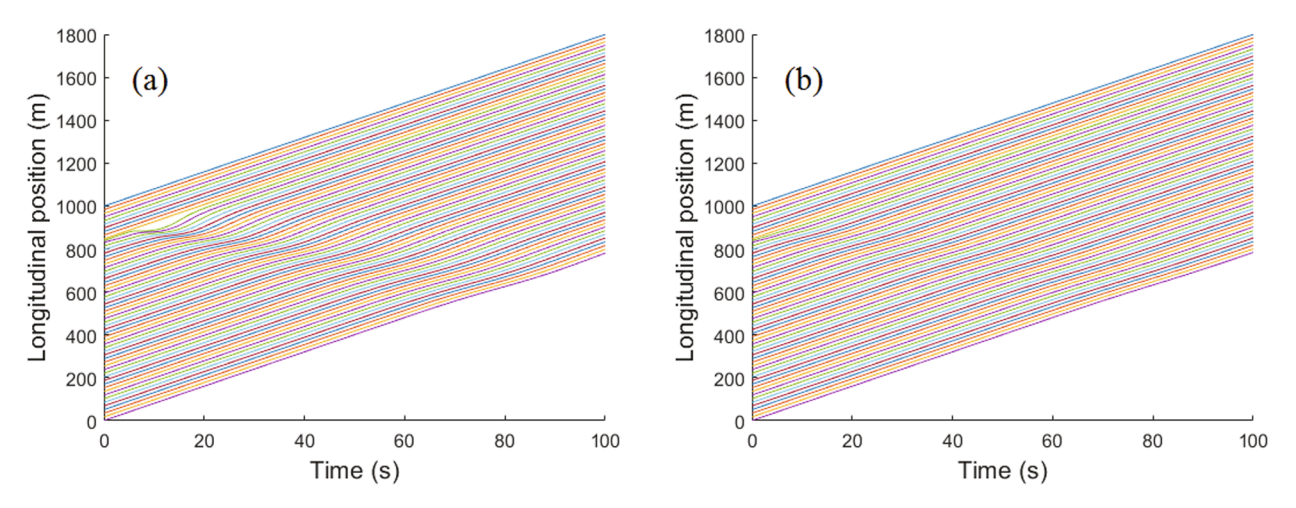


Fig. 8. Time-space diagram of all vehicles produced by (a) the TLCM, and (b) the CLCM in a representative scenario.

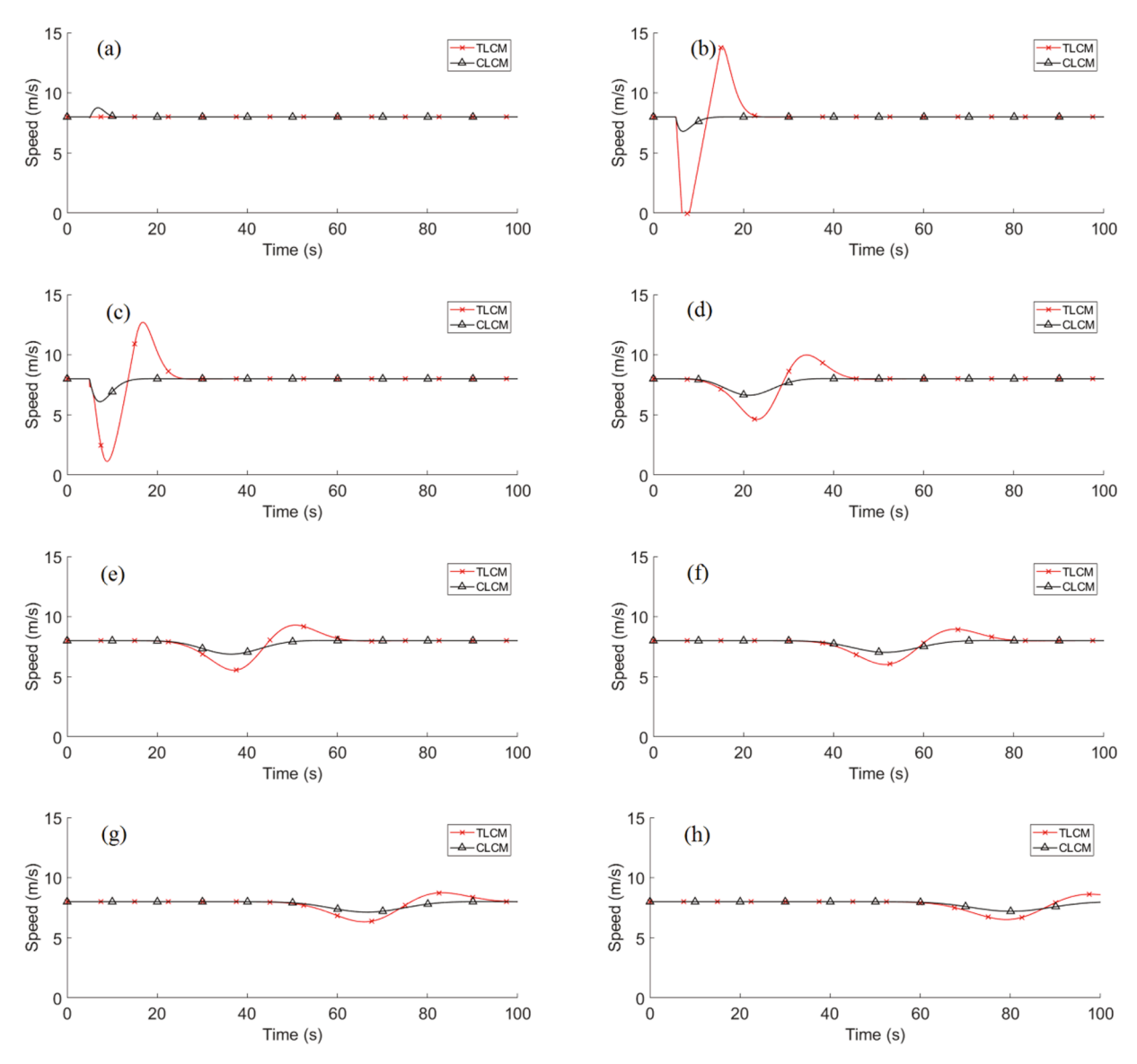


Fig. 9. Speed evolutions of the (a) PV, (b) SV, (c) first, (d) eleventh, (e) twenty first, (f) thirty first, (g) forty first, and (h) fiftieth vehicle in the upstream traffic.

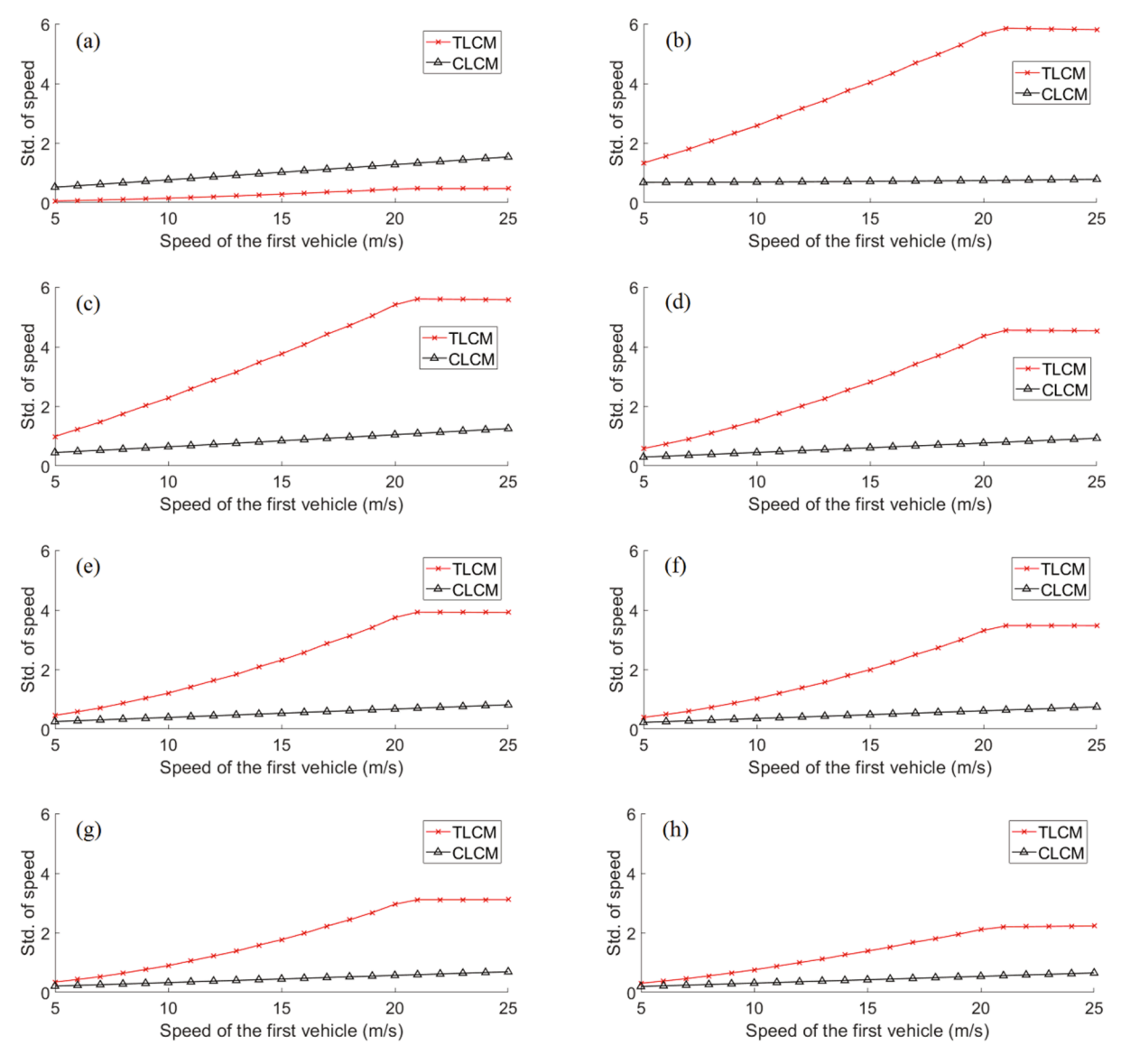


Fig. 10. Standard deviations of the speed of the (a) PV, (b) SV, (c) first, (d) eleventh, (e) twenty first, (f) thirty first, (g) forty first, and (h) fiftieth vehicle in the upstream with varying speed of the first vehicle on the target lane.

$$y_{SV}(x_{SV}(t_m^S)) = \tan(\theta(t_m^S)), \forall m \in \mathcal{M};$$
 (38)

$$y_{SV}(x_{SV}(T|m)) = 0, \forall m \in \mathcal{M}.$$
(39)

Solving the above equations yields an analytical solution to the parameters in Eq. (35) as follows

$$-\frac{\left(y_{SV}\left(r_{m}^{S}\right)+L\right)\left(3x_{SV}\left(r_{m}^{S}\right)^{2}x_{SV}(T|m)-x_{SV}\left(r_{m}^{S}\right)^{3}\right)}{\left(x_{SV}\left(r_{m}^{S}\right)-x_{SV}(T|m)\right)\left(x_{SV}\left(r_{m}^{S}\right)^{2}-2x_{SV}\left(r_{m}^{S}\right)x(T|m)+x_{SV}(T|m)^{2}\right)},\forall m \in \mathcal{M};$$
(40)

$$k_{6}(m) = \frac{\left(x_{\text{SV}}\left(t_{m}^{\text{S}}\right) - x_{\text{SV}}(T|m)\right)\left(3y_{\text{SV}}\left(t_{m}^{\text{S}}\right)x_{\text{SV}}(T|m)^{2} - x\left(t_{m}^{\text{S}}\right)x_{\text{SV}}(T|m)^{2} \tan\left(\theta\left(t_{m}^{\text{S}}\right)\right)\right)}{\left(x_{\text{SV}}\left(t_{m}^{\text{S}}\right) - x_{\text{SV}}(T|m)\right)\left(x_{\text{SV}}\left(t_{m}^{\text{S}}\right)^{2} - 2x_{\text{SV}}\left(t_{m}^{\text{S}}\right)x(T|m) + x_{\text{SV}}(T|m)^{2}\right)}$$

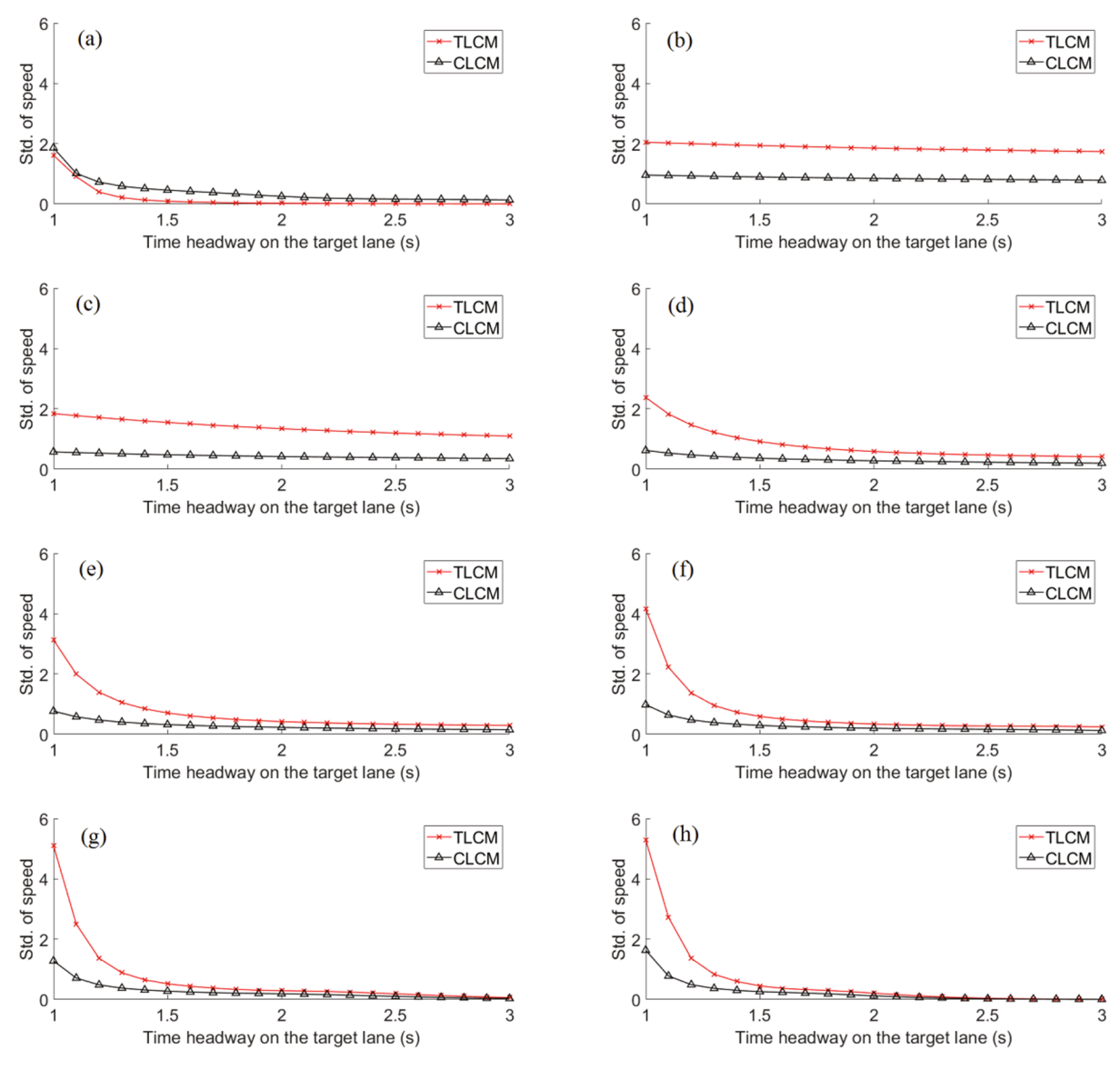


Fig. 11. Standard deviations of the speed of the (a) PV, (b) SV, (c) first, (d) eleventh, (e) twenty first, (f) thirty first, (g) forty first, and (h) fiftieth vehicles in the upstream with varying initial time headway between each two consecutive vehicles on the target lane.

$$k_{5}(m) = \frac{-\left(x_{SV}(T|m)\left(\tan\left(\theta\left(t_{m}^{S}\right)\right)\left(x_{SV}(T|m)^{2} - 2x_{SV}\left(t_{m}^{S}\right)^{2}\right) + x_{SV}\left(t_{m}^{S}\right)\left(x(T|m)\tan\left(\theta\left(t_{m}^{S}\right)\right) - 6L\right)\right)\right)}{\left(x_{SV}\left(t_{m}^{S}\right) - x_{SV}(T|m)\right)^{3}}, \forall m \in \mathcal{M};$$

$$(41)$$

$$k_{4}(m) = \frac{x_{SV}(T|m)\left(2x_{SV}(T|m)\tan\left(\theta\left(t_{m}^{S}\right)\right) - 3L\right) - x_{SV}\left(t_{m}^{S}\right)\left(L + \left(x_{SV}\left(t_{m}^{S}\right) + x_{SV}(T|m)\right)\right)}{\left(x_{SV}\left(t_{m}^{S}\right) - x_{SV}(T|m)\right)^{3}}, \forall m \in \mathcal{M};$$

$$(42)$$

$$k_3(m) = \frac{2L + \left(x_{SV}\left(t_m^S\right) - x_{SV}(T|m)\right)\tan\left(\theta\left(t_m^S\right)\right)}{\left(x_{SV}\left(t_m^S\right) - x_{SV}(T|m)\right)^3}, \forall m \in \mathcal{M}.$$
 (43)

Finally, to make sure the passengers in the SV are comfortable during the lane-changing process, we impose an upper bound to the lateral acceleration of the SV. The maximum lateral acceleration of the SV using the above cubic polynomial trajectory can be formulated as (Yang et al., 2018),

$$a_{SV}^{L}(t_{m}^{F}) = \left(v_{SV}(T|m)^{2}\right) \left| \frac{2x_{SV}(T|m)\left(\tan\left(\alpha_{SV}\left(t_{m}^{S}\right)\right)\right) - 6y_{SV}(T|m)}{\left(x_{SV}(T|m)\right)^{2}} \right|, \forall m \in \mathcal{M}.$$
(44)

If the lateral acceleration is greater than the maximum lateral acceleration $a^{\rm L,MAX}$, the lane-changing maneuver will be aborted, and the SV will continue lane keeping on the current lane.

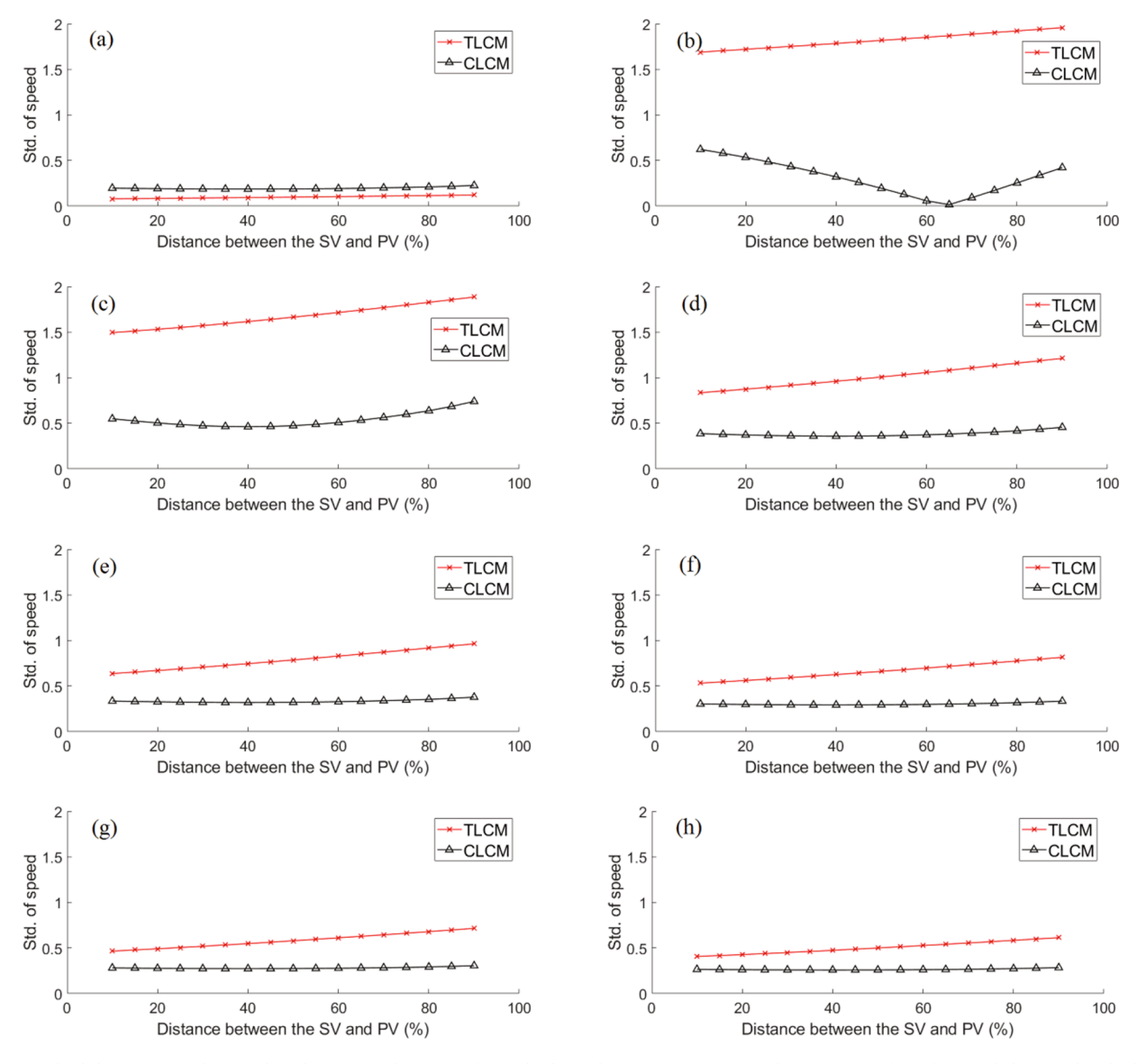


Fig. 12. Standard deviations of the speed of the (a) PV, (b) SV, (c) first, (d) eleventh, (e) twenty first, (f) thirty first, (g) forty first, and (h) fiftieth vehicle in the upstream with varying initial distance between the SV and PV.

3. Simulation and results analysis

To verify the effectiveness of the dynamic cooperative lane-changing model, we carried out extensive numerical simulations using MATLAB 2019 as the simulation platform. This section presents the simulation settings and discusses the results. We first introduce the parameter settings and the evaluation of the proposed model in terms of the success rate of lane-changing maneuvers, impacts on the study CAVs (i.e., SV, PV, and FV), and impacts on vehicles in the upstream direction of the SV's target position on the target lane will be presented successively.

3.1. Simulation settings

In the simulation, we consider a two-lane highway segment with 60 vehicles on the target lane, 10 of which are in the downstream direction of the SV's target position while 50 are in the upstream direction. The first vehicle on the target lane runs at a constant speed and other vehicles on this lane operate according to the linearized car-following model (Section 2.3.1). The simulation time horizon is 100 s and the length of each time step is 50 ms; there are 2000 time steps for each simulation. To investigate the robustness of the proposed model under different traffic

conditions, we consider four different parameters that can possibly affect the effectiveness of the proposed model, including the speed of the first vehicle on the target lane, the initial time headway between each two consecutive vehicles on the target lane, the initial distance between the SV and PV, and the initial speed difference between the SV and PV with the speed of the SV being the minuend. The speed of the first vehicle on the target lane varies from 5 to 25 m/s, with a step size of 1 m/s. The initial time headway between each two consecutive vehicles on the target lane varies from 1.0 to 3.0 s, with a step size of 0.1 s. The initial distance between the SV and PV varies from 10% to 90% of the distance between the PV and FV, with a step size of 5%. The initial speed difference of the SV and PV varies from -3 to 3 m/s, with a step size of $0.5 \, m/s$. With this setting, we created 97,461 scenarios with different initial conditions for the simulation analysis. Other parameters used in the simulation remain constant across all scenarios and are summarized in Table 2.

Further, to demonstrate the effectiveness of the proposed lanechanging model with the acceleration-deceleration paradigm, we compare the results of the proposed cooperative lane-changing model (CLCM) with a traditional lane-changing model (TLCM) where the deceleration-only paradigm is implemented (Wang et al., 2020). The

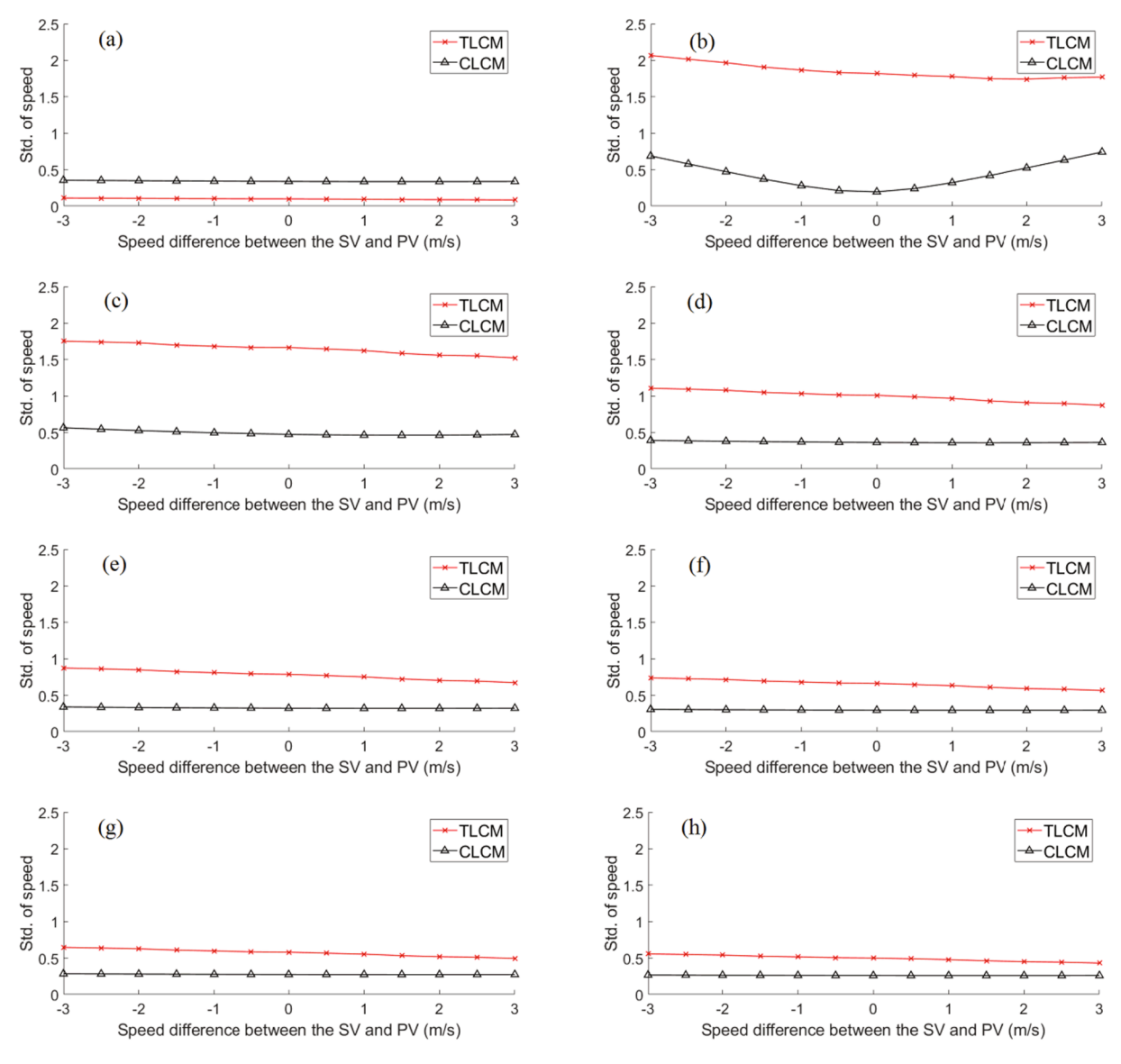


Fig. 13. Standard deviations of the speed of the (a) PV, (b) SV, (c) first, (d) eleventh, (e) twenty first, (f) thirty first, (g) forty first, and (h) fiftieth vehicle in the upstream with varying initial speed difference of the SV and PV.

effectiveness of both models is assessed from three aspects, namely the success rate of lane-changing maneuvers, impacts on the study CAVs (i. e., the PV, SV, and FV), impacts on the vehicles in the upstream direction of the target position of the SV (we call them the upstream vehicles hereafter for the simplicity of the illustration). The success rate of the lane-changing maneuvers is defined as the ratio of the number of scenarios where the SV successfully changes its lane to the number of scenarios. To investigate the impacts of the lane-changing process on the traffic operations, we plot the speed profiles of the study CAVs and upstream CAVs in some representative scenarios to present whether there is a speed variation. Further, we use the standard deviation of the speeds of these vehicles as a measure to quantitatively analyze these impacts under various parameter settings.

3.2. Success rate of lane-changing maneuvers

The success rates of both models out of all simulated scenarios are summarized in Table 3. The success rates of lane-changing maneuvers with varying parameter settings are presented in Fig. 5. Subplots provide results with varying speed of the first vehicle on the target lane (a), varying initial time headway between each two consecutive vehicles on

the target lane (b), varying initial distance between the SV and PV (c), and varying initial speed difference between the SV and PV (d). The trajectories of the PV, SV, FV during the lane-changing process in one simulated scenario are presented in Fig. 6.

As can be seen from Table 3, out of 97,461 scenarios, the SV successfully takes lane-changing maneuvers 51,752 times (with a success rate of 53.1%) with the TLCM while this value increases to 70,756 (with a success rate of 72.6%) with the CLCM. The CLCM results in an increase of 36.7% in terms of the success rate of the lane-changing maneuvers. This result shows that the coordination between the SV and its surrounding vehicles during the lane-changing process creates more opportunities for the SV's lane-changing maneuvers. Fig. 5 further reveals how this improvement changes with different input parameters. We see from Fig. 5(a) that with the increase in the speed of the first vehicle on the target lane, the success rate declines in both models because the increasing speed requires a longer distance between the PV and FV for the SV to change lane. However, the success rate of the CLCM is consistently higher than that of the TLCM despite the variations in the speed of the first vehicle on the target lane. Fig. 5(b) shows similar results, with the success rate of the CLCM greater than that of the TCLM except when the time headway between each two consecutive vehicles is greater than 2.5 s. However, CLCM results in the same success rates as TLCM when improvements are not obtained, indicating that CLCM at least performs as well as TLCM. Interestingly, the success rate of the TLCM is 0% when the time headway is less than or equal to 1.6 s. This observation indicates that the SV cannot take lane-changing maneuvers at all in this condition because the time headway between each two consecutive vehicles on the target lane is so small that there is not enough space for the SV's lane-changing maneuvers. This situation is changed by the CLCM; with the acceleration of the PV, enough space is provided for the SV to change its lane in around 30% of the simulated scenarios. This result implies that the proposed CLCM is particularly important for corridors with congested traffic where the time headway between vehicles is likely to be small and thus lane changing is almost impossible with the TLCM. Fig. 5(c) and Fig. 5(d) reveal that CLCM increases the success rate of lane-changing regardless of the variations in the initial distance between the SV and PV and the initial speed difference of the SV and PV, respectively. Further, the success rate of lanechanging maneuvers is not affected by the variations in these two parameters in both models.

Fig. 6 visualizes the trajectories of the PV, SV, and FV during the lane-changing process with vehicles in dashed lines denoting the initial positions and vehicles in solid lines representing the final positions. As can be seen from this figure, the SV is able to commence the lane-changing maneuver with a smooth trajectory without colliding with the SV and FV. These results prove that our proposed model is able to conduct safe and comfortable lane-changing maneuver for CAVs.

3.3. Impacts on the study CAVs

The speed evolutions of the study CAVs in two representative scenarios are presented in Fig. 7. The standard deviations of the speed of the PV and SV versus varying speed of the first vehicle on the target lane, varying initial time headway between each two consecutive vehicles on the target lane, varying initial distance between the SV and PV, and varying initial speed difference of the SV and PV are presented in Fig. 10 (a)-(b), Fig. 11 (a)-(b), Fig. 12 (a)-(b), Fig. 13 (a)-(b), respectively.

As seen from Fig. 7, the SV suffers from an evident speed oscillation with an amplitude of 8 m/s and even a complete stop for about 2 s in the TLCM. This phenomenon, however, is alleviated in the CLCM, with its amplitude decreased to 3 m/s, since the SV does not have to decelerate as much with the cooperative behavior of the PV and FV. In addition, the SV's adjustment time for lane changing decreases from 20 s (TLCM) to 10 s (CLCM). Further, the SV's lane-changing maneuvers inevitably affect the operation of the FV in both models, but the impact in the CLCM is not as significant that in the TLCM. The PV's speed remains constant during the lane-changing process in the TLCM, while a small speed oscillation of the PV is observed in the CLCM in the second case (see Fig. 7(d)). This is because, in the proposed model, the PV may accelerate to cooperate with the SV's lane-changing maneuvers. However, the magnitude of the oscillation reduction in other vehicles (including the SV, FV and other vehicles in the upstream direction that will be discussed in the next subsection) is far greater than the magnitude of the oscillation increase in the PV, meaning that the increase in the PV's speed oscillation can be completely offset by the decrease in other vehicles' speed oscillations. Thus, the proposed model still reduces the negative impacts of lane-changing maneuvers on the traffic operation from a system perspective.

The same phenomenon is also observed in other scenarios with different parameter settings shown in Fig. 10, Fig. 11, Fig. 12, and Fig. 13. We see that the standard deviations of the PV's speed in the CLCM are generally greater than those in the TLCM, indicating the CLCM causes the PV a greater speed oscillation than the TLCM. However, the amplitude of this oscillation (which can be measured by the gap between the two curves in the same subplot) is obviously much smaller than the sum of the amplitude of other vehicles' speed oscillation. Thus, the CLCM consistently reduces the traffic disruptions in the

investigated highway system in a variety of parameter settings.

3.4. Impacts on the upstream vehicles

The time–space diagrams of the vehicles in one of the simulated scenarios from the CLCM and TLCM are presented in Fig. 8. The speed evolutions of the first, eleventh, twenty first, thirty first, forty first, and fiftieth vehicles in the upstream in the same scenario are presented in Fig. 9 (c)-(h). The standard deviations of the speed of these vehicles versus varying speed of the first vehicle on the target lane, varying initial time headway between each two consecutive vehicles on the target lane, varying initial distance between the SV and PV, and varying initial speed difference of the SV and PV are presented in Fig. 10 (c)-(h), Fig. 11 (c)-(h), Fig. 12 (c)-(h), Fig. 13 (c)-(h), respectively.

As can be seen in Fig. 8(a), there is a shockwave starting at the 10-th second and propagating along the upstream vehicles when the TLCM is applied to design the lane-changing maneuvers. The CLCM model, however, causes almost no observable shockwave among the upstream vehicles, as shown in Fig. 8(b). This result indicates that with proper coordination, the CLCM can alleviate the disruption in the upstream traffic flow caused by the SV's lane-changing maneuvers. Fig. 9(c)-(h) offer a more intuitive presentation of this impact. As can be seen from Fig. 9(c)-(h), all the selected vehicles experience an evident speed oscillation when TLCM is applied. While there are also observable speed oscillations in these vehicles with the CLCM, the amplitudes of these oscillations are much smaller and thus brings almost no substantial impacts on the traffic operation. This result is consistent with the fact that there is no observable shockwave in the time-space diagram in Fig. 8(b). These results reveal that the CLCM alleviates the negative impacts of lane-changing maneuver on the upstream traffic flow compared with TLCM.

As can be seen from Fig. 10 (c)-(h), the standard deviations of the selected vehicles' speeds increase with the increase in the speed of the first vehicle on the target lane. The speed variations of all selected vehicles produced by CLCM are much lower than those produced by TLCM, indicating that the CLCM consistently produces smoother trajectories for the upstream vehicles than the TLCM. Further, the gap between the lines in all subplots becomes larger as the speed of the first vehicle on the target lane increases until it reaches $20\ m/s$, meaning that the proposed CLCM's capability in reducing traffic oscillations in the upstream traffic flow is stronger when the speed of the first vehicle on the target lane is higher. Also, we observe that the standard deviations of the speed decrease as the vehicle number increases (i.e., from Fig. 10 (c) to (h)), which indicates that the shockwave is dampened gradually along the upstream traffic direction.

Fig. 11 (c)-(h) show that with the increase in the time headway between each two consecutive vehicles on the target lane, the standard deviations of each selected CAV's speed decrease in both lane-changing models. Further, the standard deviations of the first thirty vehicles in the target lane produced by the CLCM is always smaller than those produced by the TLCM, with the difference being very substantial when the time headway value is small. This observation indicates that the proposed CLCM smoothens the trajectories of the first thirty vehicles with all considered time headway values. For the remaining vehicles, trajectory smoothing is still achieved when the time headway is small (as shown by the gap between the two curves in Fig. 11 (g)-(h)). Also, when improvement is not observed, CLCM performs as well as TLCM, which is similar to the impacts of this input parameter on the success rate of the lane-changing maneuvers.

The impact on upstream CAVs' speed standard deviation of the initial distance between the SV and PV is shown in Fig. 12 (c)-(h). The CLCM achieves smaller speed standard deviations than the TLCM in all upstream CAVs. Interestingly, the speed standard deviations of the first 41 CAVs in the upstream direction is first getting smaller and then larger as the initial distance between the SV and PV increases when the CLCM is applied, as seen by the U-shape curves for the CLCM in Fig. 12 (c)-(f).

However, the speed standard deviations of these vehicles are strictly increasing as the initial distance between the SV and PV increases when the TLCM is applied. This is because, when the initial distance between PV and SV is small, the acceleration of the PV cannot provide enough space for the SV's lane-changing maneuvers, and thus the SV must decelerate to maintain a safety distance. As a result, the FV and the following vehicles are affected. As the initial distance between the PV and SV gets larger, the impacts of the SV's deceleration on the upstream vehicles are reduced, thus leading to a decreasing standard deviation of their speeds. Yet, when the initial distance between the SV and PV reaches 60% (i.e., the initial distance between the SV and FV is less than 40%), even though the acceleration of the PV provides more space for the SV, the FV still needs to decelerate relatively more to avoid collisions because of its short distance to the SV. This impact gets stronger as the initial distance between the SV and PV gets smaller, thus bringing a more substantial speed oscillation. In contrast, the space necessary for the SV's lane-changing maneuvers is only provided via the FV's deceleration in the TLCM, so the resulting speed standard deviations are more evident. Further, the FV has to accelerate more as the initial distance between the PV and SV gets larger, and thus a higher speed standard deviation is witnessed. These results, again, indicate the CLCM is effective in smoothing trajectories of the following CAVs.

Finally, Fig. 13 (c)-(h) show how the initial speed difference between SV and PV affects the speed standard deviation of the CAVs in the upstream direction. Again, it can be seen that CLCM consistently decline the standard deviations of the speeds of the upstream CAVs with different values of the initial speed difference between the SV and PV. Furthermore, the gaps between the two curves in each subplot decrease as the parameter value increases, showing that the effectiveness of the CLCM in reducing the disruptions of the SV's lane-changing maneuvers in the upstream CAVs is weakened as the initial speed difference between the SV and PV increases.

4. Conclusion and future work

This study proposes a dynamic cooperative lane-changing model for CAVs with possible accelerations of a preceding vehicle. This model is designed to make lane-changing decisions for the SV and generate trajectories for the SV, PV, and FV in a coordinated manner dynamically. The lane-changing decision is made by analytically analyzing vehicle kinematics given the states of the SV, PV, and FV, the minimum safety distance, and requirements on the comfort level for passengers. The longitudinal and lateral trajectories of the vehicles are designed with a linear car-following model and a cubic polynomial curve method, respectively. Results from numerical simulation in extensive scenarios show that the proposed model is effective in coordinating the maneuvers of the SV, PV, and FV during the lane-changing process. It substantially increases the success rate of the SV's lane-changing maneuvers since the possible acceleration of the PV brings a higher probability of obtaining the required space for lane changing. Furthermore, the trajectories of the SV and all vehicles scattered in the upstream direction of the SV's target position on the target lane are smoothened and thus the traffic disruption (or shockwave) is much alleviated. Although the PV's speed experiences a slightly greater oscillation since it may accelerate to make space for the SV's lane-changing maneuvers, the oscillation reduction in other vehicles completely offsets this small increase in the PV's speed oscillation. Therefore, the proposed model still achieves a system-wide improvement in terms of reducing the negative impacts of lanechanging maneuvers on the traffic operation. In addition, results confirm the effectiveness of the proposed model under a variety of parameter settings corresponding to various traffic conditions in the real world.

This study adds to the body of literature demonstrating the necessity of adopting cooperative centralized control in lane-changing decisions for CAVs. Further, the model presented here provides a simple yet powerful analytical tool that can be used in future CAV studies and planning practice. Results show that the traffic oscillation of the PV is amplified in the proposed model, future research may integrate a trajectory optimization component to search for the optimal trajectory of the vehicles so that this amplification can be minimized. Also, this study investigates the case where only one SV needs to change lane and can be used as a foundation for developing sophisticated models for a more complicated case where multiple lane-changing requests need to be answered. Development of such a model requires an integrated perspective from the entire system, which will be an interesting research direction. Further, this study regards the CAV's willingness to cooperate as a deterministic input acquired via V2V communication. Yet, a CAV's willingness to cooperate may depend on various subjective factors, e.g., the passengers' perception of the resultant delay, the presence and attractiveness of the incentives, the passengers' personality. Further studies can extend this work to incorporate the effects of these factors on the willingness to cooperate into the model with a fuzzy modeling approach (e.g., Martín et al., 2016). Finally, apart from the lanechanging problem considered in this study, the lane-changing behavior on a two-lane road where on each lane the vehicles travel in opposite directions is also interesting and important. Yet, the analysis of the latter is more complex since it would require a consideration of the vehicle movements in the opposite direction. Future studies can base on this study to propose lane-changing models for the more complicated

CRediT authorship contribution statement

Zhen Wang: Conceptualization, Methodology, Software, Writing original draft. Xiangmo Zhao: Conceptualization, Project administration, Resources, Investigation, Funding acquisition. Zhiwei Chen: Conceptualization, Methodology, Writing - original draft, Formal analysis, Validation. Xiaopeng Li: Conceptualization, Supervision, Resources, Funding acquisition.

Declaration of Competing Interest

The authors declare that they have no known competing financial interests or personal relationships that could have appeared to influence the work reported in this paper.

Acknowledgements

This work is partially supported by the Guizhou Province Science and Technology Major Project (No. ZNWLQC[2019]3012-2), National Natural Science Foundation of China (No. U1864204, 61703054). Natural Science Foundation of Shaanxi Province (No. 2018JQ6035), U.S. National Science Foundation (CMMI #1932452). '111' project (No. B14043). Mr. Zhen Wang greatly acknowledges financial support from China Scholarship Council.

References

Ammoun, S., Nashashibi, F., & Laurgeau, C. (2007). An analysis of the lane changing manoeuvre on roads: the contribution of inter-vehicle cooperation via communication. 1095–1100.

Fagnant, D. J., & Kockelman, K. (2015). Preparing a nation for autonomous vehicles: Opportunities, barriers and policy recommendations. *Transportation Research Part A*, 77, 167–181. https://doi.org/10.1016/j.tra.2015.04.003

Ganji, B., Kouzani, A. Z., Khoo, S. Y., & Shams-Zahraei, M. (2014). Adaptive cruise control of a HEV using sliding mode control. Expert Systems with Applications, 41(2), 607–615. https://doi.org/10.1016/j.eswa.2013.07.085

Ghasemi, A., Kazemi, R., & Azadi, S. (2013). Stable Decentralized Control of a Platoon of Vehicles With Heterogeneous Information Feedback. *IEEE Transactions on Vehicular Technology*, 62(9), 4299–4308. https://doi.org/10.1109/TVT.2013.2253500

González, D., Pérez, J., & Milanés, V. (2017). Parametric-based path generation for automated vehicles at roundabouts. Expert Systems with Applications, 71, 332–341. https://doi.org/10.1016/j.eswa.2016.11.023

Hou, Y., Edara, P., & Sun, C. (2015). Situation assessment and decision making for lane change assistance using ensemble learning methods. Expert Systems with Applications, 42(8), 3875–3882. https://doi.org/10.1016/j.eswa.2015.01.029

- Li, B., Zhang, Y., Feng, Y., Zhang, Y., Ge, Y., & Shao, Z. (2018). Balancing Computation Speed and Quality: A Decentralized Motion Planning Method for Cooperative Lane Changes of Connected and Automated Vehicles. *IEEE Transactions on Intelligent* Vehicles, 3(3), 340–350. https://doi.org/10.1109/TIV10.1109/TIV.2018.2843159
- Li, B., Zhang, Y., Ge, Y., Shao, Z., & Li, P. (2017). Optimal control-based online motion planning for cooperative lane changes of connected and automated vehicles. IEEE International Conference on Intelligent Robots and Systems, 2017-Septe, 3689–3694. 10.1109/IROS.2017.8206215.
- Li, L., & Li, X. (2019). Parsimonious trajectory design of connected automated traffic. Transportation Research Part B: Methodological, 119, 1–21. https://doi.org/10.1016/j. trb.2018.11.006
- Li, P. (Taylor), & Zhou, X. (2017). Recasting and optimizing intersection automation as a connected-and-automated-vehicle (CAV) scheduling problem: A sequential branchand-bound search approach in phase-time-traffic hypernetwork. Transportation Research Part B: Methodological, 105, 479–506. 10.1016/j.trb.2017.09.020.
- Li, X., & Sun, J. Q. (2017). Studies of vehicle lane-changing dynamics and its effect on traffic efficiency, safety and environmental impact. *Physica A: Statistical Mechanics* and Its Applications, 467, 41–58. https://doi.org/10.1016/j.physa.2016.09.022
- Li, S. E., & Peng, H. (2012). Strategies to minimize the fuel consumption of passenger cars during car-following scenarios. Proceedings of the Institution of Mechanical Engineers, Part D: Journal of Automobile Engineering, 226(3), 419–429. https://doi. org/10.1177/0954407011420214
- Li, X., Sun, Z., Cao, D., Liu, D., & He, H. (2017). Development of a new integrated local trajectory planning and tracking control framework for autonomous ground vehicles. *Mechanical Systems and Signal Processing*, 87, 118–137. https://doi.org/ 10.1016/j.ymssp.2015.10.021
- Li, Z., Zhang, R., Xu, S., & Qian, Y. (2015). Study on the effects of driver's lane-changing aggressiveness on traffic stability from an extended two-lane lattice model. Communications in Nonlinear Science and Numerical Simulation, 24(1–3), 52–63. https://doi.org/10.1016/j.cnsns.2014.12.007
- Luo, Y., Xiang, Y., Cao, K., & Li, K. (2016). A dynamic automated lane change maneuver based on vehicle-to-vehicle communication. *Transportation Research Part C: Emerging Technologies*, 62, 87–102. https://doi.org/10.1016/j.trc.2015.11.011
- Martín, S., Romana, M. G., & Santos, M. (2016). Fuzzy model of vehicle delay to determine the level of service of two-lane roads. Expert Systems with Applications, 54, 48–60. https://doi.org/10.1016/j.eswa.2015.12.049
- Milanés, V., & Shladover, S. E. (2014). Modeling cooperative and autonomous adaptive cruise control dynamic responses using experimental data. *Transportation Research Part C: Emerging Technologies*, 48, 285–300. https://doi.org/10.1016/j. trc.2014.09.001
- Nie, J., Zhang, J., Ding, W., Wan, X., Chen, X., & Ran, B. (2016). Decentralized Cooperative Lane-Changing Decision-Making for Connected Autonomous Vehicles. *IEEE Access*, 4, 9413–9420. https://doi.org/10.1109/ACCESS.2017.2649567
- Pan, T. L., Lam, W. H. K., Sumalee, A., & Zhong, R. X. (2016). Modeling the impacts of mandatory and discretionary lane-changing maneuvers. *Transportation Research Part C: Emerging Technologies*, 68, 403–424. https://doi.org/10.1016/j.trc.2016.05.002
- Peng, T., Su, L., Zhang, R., Guan, Z., Zhao, H., Qiu, Z., ... Xu, H. (2020). A new safe lane-change trajectory model and collision avoidance control method for automatic driving vehicles. Expert Systems with Applications, 141, 112953. https://doi.org/10.1016/j.eswa.2019.112953

- Rahman, M., Chowdhury, M., Xie, Y., & He, Y. (2013). Review of Microscopic Lane-Changing Models and Future Research Opportunities. *IEEE Transactions on Intelligent Transportation Systems*, 14(4), 1942–1956. https://doi.org/10.1109/ TTIS_013_227074
- Stanković, S. S., Stanojević, M. J., & Šiljak, D. D. (2000). Decentralized overlapping control of a platoon of vehicles. *IEEE Transactions on Control Systems Technology*, 8 (5), 816–832. https://doi.org/10.1109/87.865854
- Tang, J., Liu, F., Zhang, W., Ke, R., & Zou, Y. (2018). Lane-changes prediction based on adaptive fuzzy neural network. Expert Systems with Applications, 91, 452–463. https://doi.org/10.1016/j.eswa.2017.09.025
- Tang, J., Yu, S., Liu, F., Chen, X., & Huang, H. (2019). A hierarchical prediction model for lane-changes based on combination of fuzzy C-means and adaptive neural network. Expert Systems with Applications, 130, 265–275. https://doi.org/10.1016/j. eswa.2019.04.032
- Wang, D., Hu, M., Wang, Y., Wang, J., Qin, H., & Bian, Y. (2016). Model predictive control-based cooperative lane change strategy for improving traffic flow. Advances in Mechanical Engineering, 8(2), 1–17. https://doi.org/10.1177/1687814016632992
- Wang, M., Daamen, W., Hoogendoorn, S. P., & van Arem, B. (2014a). Rolling horizon control framework for driver assistance systems. Part I: Mathematical formulation and non-cooperative systems. *Transportation Research Part C: Emerging Technologies*, 40, 271–289. https://doi.org/10.1016/j.trc.2013.11.023
- Wang, M., Daamen, W., Hoogendoorn, S. P., & van Arem, B. (2014b). Rolling horizon control framework for driver assistance systems. Part II: Cooperative sensing and cooperative control. *Transportation Research Part C: Emerging Technologies*, 40, 290–311. https://doi.org/10.1016/j.trc.2013.11.024
- Wang, M., Hoogendoorn, S. P., Daamen, W., van Arem, B., & Happee, R. (2015). Game theoretic approach for predictive lane-changing and car-following control. *Transportation Research Part C: Emerging Technologies*, 58, 73–92. https://doi.org/ 10.1016/j.trc.2015.07.009
- Wang, Z., Shi, X., & Li, X. (2019). Review of Lane-Changing Maneuvers of Connected and Automated Vehicles: Models, Algorithms and Traffic Impact Analyses. *Journal of the Indian Institute of Science.*, 99(4), 589–599. https://doi.org/10.1007/s41745-019-00127.
- Wang, Z., Zhao, X., Xu, Z., Li, X., & Qu, X. (2020). Modeling and Field Experiments on Lane Changing of an Autonomous Vehicle in Mixed Traffic. Computer-aided Civil and Infrastructure Engineering. https://doi.org/10.13140/RG.2.2.19857.58724. [In press]
- Xiao, L., & Gao, F. (2011). Practical string stability of platoon of adaptive cruise control vehicles. IEEE Transactions on Intelligent Transportation Systems, 12(4), 1184–1194. https://doi.org/10.1109/TITS.2011.2143407
- Yang, D., Zheng, S., Wen, C., Jin, P. J., & Ran, B. (2018). A dynamic lane-changing trajectory planning model for automated vehicles. *Transportation Research Part C: Emerging Technologies*, 95(June), 228–247. https://doi.org/10.1016/j. trc 2018/06/007
- You, F., Zhang, R., Lie, G., Wang, H., Wen, H., & Xu, J. (2015). Expert Systems with Applications Trajectory planning and tracking control for autonomous lane change maneuver based on the cooperative vehicle infrastructure system. Expert Systems with Applications, 42(14), 5932–5946. https://doi.org/10.1016/j.eswa.2015.03.022
- Zhang, X., & Zhu, X. (2019). Autonomous path tracking control of intelligent electric vehicles based on lane detection and optimal preview method. Expert Systems with Applications, 121, 38–48. https://doi.org/10.1016/j.eswa.2018.12.005